

# MOVEMENT AND SELF-CONTROL IN PROTEIN ASSEMBLIES

## Quasi-Equivalence Revisited

D. L. D. Caspar, *The Rosenstiel Basic Medical Sciences Research Center,  
Brandeis University, Waltham, Massachusetts 02254 U.S.A.*

**ABSTRACT** Purposeful switching among different conformational states exerts self-control in the construction and action of protein assemblies. Quasi-equivalence, conceived to explain icosahedral virus structure, arises by differentiation of identical protein subunits into different conformations that conserve essential bonding specificity. Mechanical models designed to represent the energy distribution in the structure, rather than just the arrangement of matter, are used to explore flexibility and self-controlled movements in virus particles. Information about the assembly of bacterial flagella, actin, tobacco mosaic virus and the T4 bacteriophage tail structure show that assembly can be controlled by switching the subunits from an inactive, unsociable form to an active, associable form. Energy to drive this change is provided by the intersubunit bonding in the growing structure; this self-control of assembly by conformational switching is called "autostery", by homology with allostery. A mechanical model of the contractile T4 tail sheath has been constructed to demonstrate how self-controlled activation of a latent bonding potential can drive a purposeful movement. The gradient of quasi-equivalent conformations modelled in the contracting tail sheath has suggested a workable mechanism for self-determination of tail tube length. Concerted action by assemblies of identical proteins may often depend on individually differentiated movements.

### ICOSAHERAL VIRUSES

"Quasi-equivalence" was conceived to describe ways in which large numbers of identical protein subunits could build closed containers of predetermined size such as virus capsids by a "self-assembly" process (Caspar and Klug, 1962). Self-assembly presumes specificity of bonding among the structural units. If the same contact points between neighboring units were used over and over again, in exactly the same way, identical units would be equivalently related and the completed assembly would have some kind of well-defined symmetry: this idea led to the prediction that rod-shaped viruses should have helical symmetry; and "spherical" viruses might have tetrahedral, octahedral, or icosahedral symmetry (Crick and Watson, 1956). Icosahedral symmetry, soon recognized by x-ray crystallography to be the underlying plan of some small isometric plant and animal virus particles, requires 60 and only 60 equivalent subdivisions. (Arrangement of 60 identical asymmetric units in a shell with icosahedral symmetry is illustrated in Fig. 1). By 1962 chemical studies on two small icosahedral viruses had counted more than 60 identical protein units; and electron microscopy of various icosahedral viruses had revealed regular surface arrays of morphological units not multiples or submultiples of 60. These observations posed two interrelated questions: why is icosahedral symmetry preferred? and what are the possible designs for an icosahedral capsid constructed by regular bonding of a multiple of 60 structural subunits? Anticipation of the answers to these questions was essential to their meaningful formulation.

## FULLER DOMES

Analogy between icosahedral virus particle architecture and Buckminster Fuller's "frequency modulated icosageodesic structures" (Marks, 1960) was the anticipatory key. Fuller's dome designs involve the subdivision of the surface of the sphere into nearly equivalent facets that are arranged with icosahedral symmetry (Fig. 2). If identical protein units were regularly associated one with each geodesic facet, they would then be quasi-equivalently related. Geometrically, the quasi-equivalence can be measured by the variation in size and shape of the nearly equal geodesic subdivisions; at the molecular level the same contact points between protein subunits could be used over and over again, but the units themselves or the bonds between them would have to be deformed in slightly different ways in the symmetrically distinct but quasi-equivalent positions.

### WHAT IS QUASI-EQUIVALENCE?

The idea of quasi-equivalence discards the mathematical constraint of strict equivalence while retaining the physical essentials of specificity to describe the bonding of chemically identical units. Molecular structures constructed from identical parts are not built to conform to exact mathematical concepts; rather, they must satisfy the condition that the system be in a minimum energy configuration and this may be realized by quasi-symmetric packing arrangements. Quasi-equivalence cannot, however, be expressed in any absolute terms; the decisions as to what constitutes quasi-equivalence must depend on the utility of the notion for

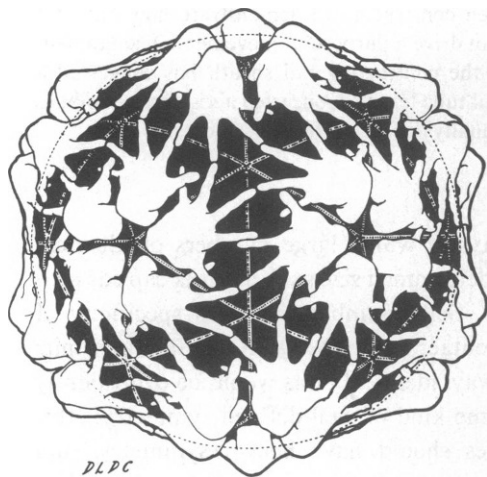


Figure 1

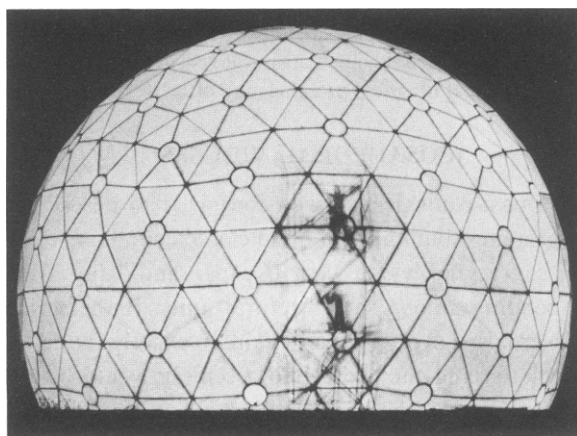


Figure 2

Figure 1 A drawing illustrating strict equivalence in a shell with icosahedral symmetry constructed from 60 identical left-handed enantiomorphic structure units. The three classes of connections possible in this surface lattice are represented by the specific bonding relations: thumb-to-pinkie - pentamer bond; ring finger-to-middle finger - trimer bond; and index finger-to-index finger - dimer bond. Any two of these three classes of bonds would hold the structure together. The underlined triangles mark out equivalent subdivisions defined by the five- and threefold axes at their vertices.

Figure 2 A Fuller Geodesic dome built on the plan of a  $T = 12$  icosahedral surface lattice. The complete circle surface would be covered by 720 of the truncated triangular facets grouped to form 12 pentamers and 110 hexamers around the small circles. Identical asymmetric structure units, as in Fig. 1, could be placed one to each facet in this surface. By bending at the joints between rigid domains of the structure units, the same specific bonding scheme shown in Fig. 1 could be preserved, but the units would then occur in 12 quasi-equivalent conformations. (Reproduced by permission of R. Buckminster Fuller.)

making predictions or for distinguishing some physically relevant invariance in the specific but nonequivalent interactions among identical units. Arrangements that minimize the variation in subunit conformation and bonding should represent minimum energy designs, assuming that optimum bonding configurations exist for isolated pairs of units that cannot all be realized by equivalent packing in any interconnected array.

### WHY ICOSAHEDRAL VIRUSES?

Our solution to the icosahedral virus capsid design problem (Caspar and Klug, 1962) involved the enumeration of all possible ways in which identical units could be connected using the same nearest neighbor contact pattern to form closed containers. These arrangements can be represented by polyhedra constructed from folded plane lattices that have sixfold or fourfold rotational symmetry. The plane hexagonal array is represented by a periodic net of equilateral triangles that join six at each lattice point and, correspondingly, the square array has four facets joined at each lattice point. All the polyhedra formed from these nets have topologically restricted numbers of vertices at which the number of triangular or square facets that meet is less than at lattice points in the plane. The range of variation of dihedral angles in these polyhedra built of equilateral triangular or square facets provides a measure of the degree of quasi-equivalence that could be realized among identical units each making the same kind of contacts with its nearest neighbors. Another way to represent these container designs is to project the polyhedra faces onto the surface of a sphere adjusting edge lengths and facet areas to minimize the variations. In whatever way the geometric comparisons are made, the icosahedral surface lattices derived from the folding up of a plane equilateral triangular net have the smallest range of variation among their quasi-equivalently related parts of all surface lattices consisting of the same or similar number of parts. This answers the question as to the selective advantage of the icosahedral designs for closed containers built of a large number of specifically bonded, identical subunits.

### ICOSAHEDRAL DESIGNS ENUMERATED

Enumeration of all the possible designs for icosahedral surface lattices was derived by considering the ways in which the equilateral triangular net can be folded into polyhedra with icosahedral symmetry (called icosadeltahedra). The vector between a neighboring pair of fivefold vertices of any icosadeltahedron must be a lattice vector of the equilateral triangular net. Since the 12 fivefold vertices are equivalent, the indices  $(h,k)$  of all the vectors in the plane net that connect a lattice point chosen as origin with another lattice point  $(h,k)$  (where  $h$  and  $k$  are any pair of positive integers including zero) define all the possible icosahedral surface lattice designs; this way of counting is complete and nonredundant (Goldberg, 1937; Caspar and Klug, 1963). The triangulation numbers  $T = (h^2 + hk + k^2)$  designate the number of symmetrically distinct but quasi-equivalent situations for the 60T structural units required to build the corresponding icosahedrally symmetric shell. Units designed to build a particular icosahedral surface lattice have the potential to self-assemble, since under appropriate environmental conditions the completed shell will represent a state of minimum free energy.

### "ASSEMBLY-BY-CHILD"

A precursor to our self-assembly concept was the allegorical notion of "assembly-by-child" formulated circa 1955 by F.H.C. Crick (cf., Crick and Watson, 1956): an efficient Nature

would design the parts of a virus particle (or other regular macromolecular assembly) such that given an appropriate model of the parts a child could put them together in only one way. That a child could do it as with a toy suggested a reversible process in which the intermediate stages of construction would be simply incomplete portions of the final structure. It was misplaced faith in the childish simplicity of Nature that led us to anticipate that if we could see the completed structure in all its molecular detail, we would then be able to figure out how to take it apart and how to put it back together again the way Nature did: "The recognition that a virus can be constructed by a sub- or even self-assembly process implies that the building rules by which it is constructed can be deduced from the properties of the finished product" (Caspar and Klug, 1962). This pronouncement was, however, contradicted in the paper in which it appears by our theory of quasi-equivalence in the design of icosahedral virus shells. Since the protein units are presumed to be all created equal, they must differentiate at some stage to take up their quasi-equivalent conformations. Scrutiny of the differences among quasi-equivalent units in the completed structure may not reveal much about how these structurally crucial movements actually took place.

### KABUL DOME

The allegory of "assembly-by-child" may be relevant to some biological construction processes even when the idea of "self-assembly" may be inapt. For example, the quasi-equivalent parts of an icosahedral capsid could be differentiated during their formation to facilitate routine assembly. An analogous situation occurred in 1956 when the U.S. Department of Commerce decided at the last moment to set up a Fuller Geodesic dome as its pavilion at the International Trade Fair in Kabul, Afghanistan to compete with the more substantial Russian and Chinese pavilions (Marks, 1960). Within a few weeks the dome, designed for unskilled assembly, was manufactured, packaged, and shipped in a single plane to Kabul. Directed by one Geodesic engineer, untrained Afghan laborers attached blue-ended parts to other parts with blue ends and red with red, etc.; 48 h later the workmen had assembled all the parts into a great 100-ft diam Fuller dome—a center of attraction at the fair that the Afghans regarded as a modern technological version of the native Mongolian yurt. The irony in the comparison of this event with the current impact of Soviet military technology in Kabul focuses on a dark facet of a global tragedy, but this does not illuminate the assembly problem. Biologically relevant aspects of the Kabul dome are: the economy of its construction from identical copies of a few types of subunits that are coded to fit together in a predetermined way; and the efficiency of its assembly that required only minimal supervision to avoid or correct mistakes.

### CRANE ASSEMBLY LINE

Earlier Crane (1950) drew the analogy between the assembly mechanisms in a living cell and the mass production line of a factory. In both cases a subassembly process is utilized to make complex products out of smaller components that are separately fabricated and then associated, following definite patterns. In the factory unskilled hands can be employed since each worker has only a small job to perform, and the system provides for inspection so that imperfect products can be rejected at each level of assembly. Surveillance is employed as a control mechanism for many vital processes, as in the immune system to destroy potentially neoplastic cells; and well-tested patterns are followed to direct growth and reproduction, as in

protein synthesis and replication of nucleic acids. In contrast, the assembly of virus particles and cellular structures of comparable complexity may proceed without external control. For these structures the assembly process is different from that of a factory in that the directions for their construction are built into their constituent components. It is these biological structures that are constructed by a self-assembly process.

## 1962 SELF-ASSEMBLY MODEL

In 1962 we illustrated the idea of self-assembly with a "dynamic" model consisting of wooden peg subunits designed to assemble in the  $T = 3$  icosahedral surface lattice (Caspar and Klug, 1962). This model is shown partially and completely assembled in a series of photographs (Figs. 3 and 4) that were to have appeared in a proleptically referenced but unpublished paper on Design and Construction of Icosahedral Viruses. The mechanics of this model can be viewed more critically now than when it was constructed 18 yr ago. Charles Ingersoll, Sr. made the parts to give substance to what I saw as the essential structural demands: all the units should be the same within reasonable tolerances; each unit should have three types of specific (actual or potential) complementary bond sites that could form symmetric dimers, trimers, and both hexamers and pentamers; the geometrical relation of the three classes of bonds should allow formation of a regular plane hexagonal lattice if the bonds were confined to a single plane; the bonds at different levels should, however, require that the units aggregate in a curved rather than a plane surface; the curvature should correspond to that of the  $T = 3$  icosahedral surface lattice which can be defined by the ideal angles between the axes of a pair of hexamers ( $41^\circ 49'$ ) and a hexamer-pentamer pair ( $37^\circ 23'$ ). The key property for assembly in a closed shell of predetermined size is built-in curvature. This property is well-displayed by the different stages of assembly and misassembly shown in Fig. 3 and in the different views of the completed shell in Fig. 4. This model shows that it is possible to design a single unit with specific bond sites that can be switched by interaction with identical copies of itself to bond in the three different environments of the  $T = 3$  icosahedral surface lattice.

Plant and bacterial viruses built on the  $T = 3$  icosahedral plan have been taken apart and put back together again (Bancroft, 1970; Hohn and Hohn, 1970). Under some conditions the protein subunits can be assembled in the  $T = 1$  plan, in other situations aberrant tubular or multiple shell aggregates are formed, and in many cases the protein is reassembled into the  $T = 3$  capsid. For these simple icosahedral viruses there is still very little known about the nature of the mechanisms regulating their assembly (Casjens and King, 1975). In the assembly of tobacco mosaic virus (TMV), the single structural protein subunit can pass through an almost bewildering number of intermediate states before settling down with its nucleic acid. By analogy with TMV, the control mechanisms for icosahedral virus assembly suggested by the model in Figs. 3 and 4 are expected to be too simple. Nevertheless, the model does display some of the essential interaction properties of a structure unit designed to form an icosahedral capsid.

## MODEL-BUILDING STRATEGIES

The model shown in Figs. 3 and 4 also illustrates some general ideas about how to design mechanical analogs to represent the dynamics of macromolecular assemblies. The objective of such models is to illustrate how the functionally significant energy of interaction is distributed in the structure rather than just the way the matter is arranged. Two policies that have proved

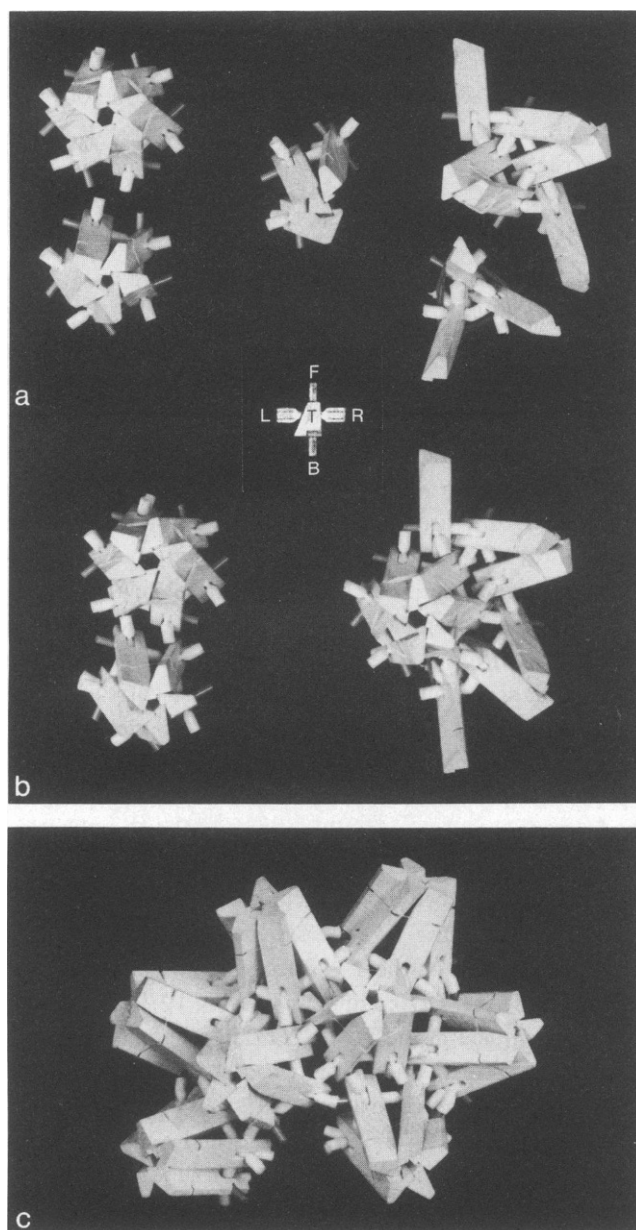


**Figure 3** Parts of the 1962 "self-assembly" model. (a) On the left: a pentamer and hexamer; center, part of a hexamer or pentamer; right, a trimer and two trimers bonded together. (b) The same units with more bonds formed. One structure unit consists of the wooden peg with a two arm plastic connector fastened to it by a short stick. The diagram in the center represents a top view (T) of a structure unit with coding of the arbitrarily defined parts: L - left-arm socket; F - front end of stick; R - right arm socket; B - back of stick. The specific bonding connections between pairs of units are: front end of stick of one unit into right arm socket of next is a trimer bond; back end of stick of one unit into left arm socket of next is a hexamer or pentamer bond; hexamer - pentamer bonds are also formed at the top of the peg by fitting the left-back corner of one unit into the notch at the right-back side of the next. Implicit bonds between bottom portions of the pegs in the assembled model are: contact between a pair of units at the base of their right-back corners corresponds to a dimer bond; contact of three units at the base of their front corners corresponds to trimer bonds. (c) Misassembly of eight pentamers attempting to form a  $T = 1$  shell. A closed shell of 12 pentamers can not be completed because the "built-in-curvature" of the structure unit will not allow the angle between pairs of pentamers to be as large as the  $63^{\circ} 26 \text{ min}$  angle required for the  $T = 1$  design.

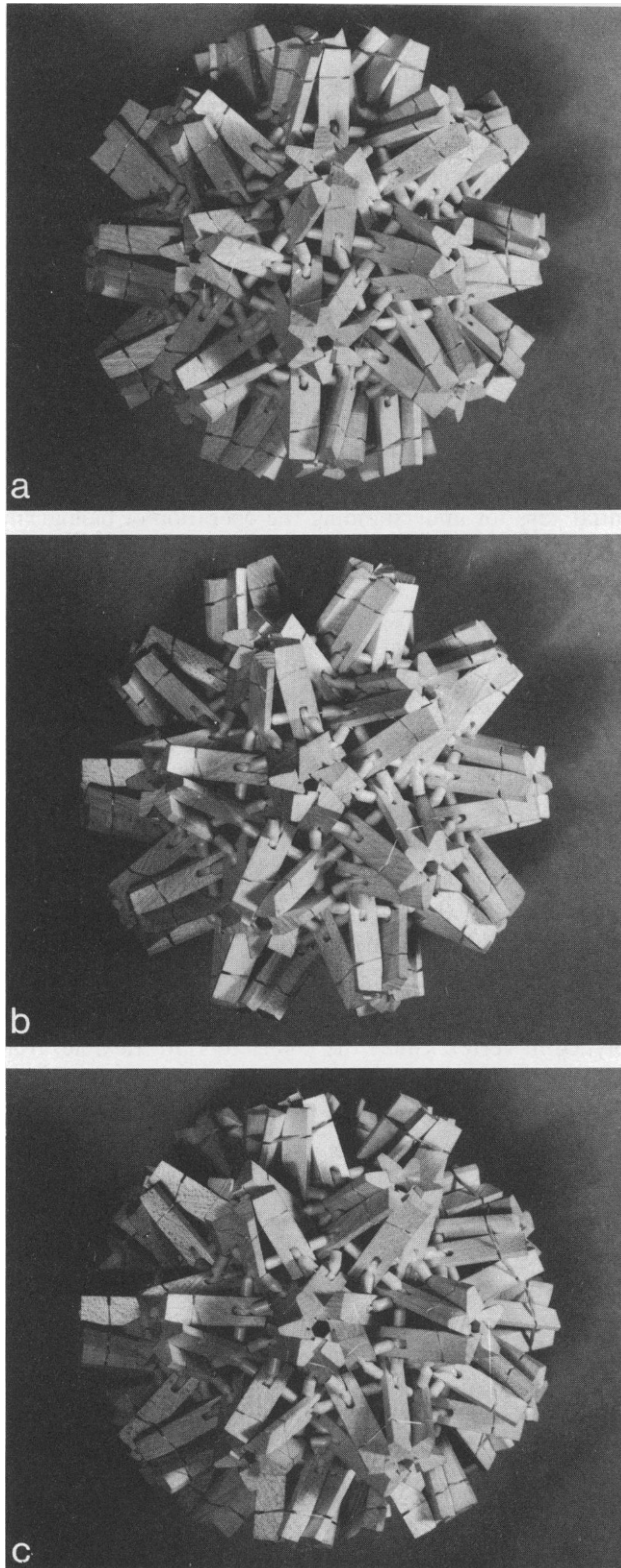


**Figure 4** Completed T - 3 "self-assembly" model viewed down: (a) Twofold axis. (b) Fivefold axis. (c) Threefold axis. A twofold axis is vertical and the model is rotated to the right about this axis from top to bottom. The hexamer bonds at the top ends of the pegs are different from (but quasi-equivalent to) the corresponding pentamer bonds. The bonding in the main framework of the model is formed by the connection between the sticks and the arm sockets. These bonds are the same for each structure unit in the three quasi-equivalent environments. Thus, there are three quasi-equivalent conformations of the structure unit at this level that differ in the flexible connection between the two arm socket domains, the stick domain, and wooden peg domain. The architecture of the stick and arm socket connection is exposed in Fig. 5.

constructive in mechanical model building are: (a) adapt pre-existing components or construction technologies whenever possible, and (b) underdesign. Underdesign does not necessarily imply an indeterminate structure, although this is often a desirable goal. Underdesign is difficult to achieve unless the construction starts with some adaptation of pre-existing components or very easily made trial pieces. If all the critical parameters are accurately fixed and the tolerances in construction are high, a model fabricated directly from raw materials can realize the intended representation but little may be learned in the construction process. A more common consequence of starting from scratch with a detailed design is the production of an overdetermined structure that is mechanically unsound or unworkable. A practical goal in mechanical model building is to try to learn more about how a biological structure may work when one starts without a very clear idea of how to build a working model. This goal may be realized by some trial-and-error construction process. This, in fact, is Nature's way for adaptation and evolutionary development. Analogies with human technology and behavior have provided essential keys for understanding the operation of biological systems (Lorentz, 1974; Atkinson, 1977) and, conversely, analogizing Nature's methods is a natural way to make analogs of Nature's machines.

### BUILDING THE 1962 MODEL

Charles Ingersoll, Sr. worked out a simple fabrication scheme to mass produce the wooden peg units seen in Figs. 3 and 4. First the general shape of the peg and the method of attachment to the underlying network were decided; then a few trial units were made and these prototypes were progressively modified until a design was found that required only half a dozen operations to produce a suitably asymmetric, interlocking piece. The framework that provides most of the actual bonding was made by fastening Geodestix components together rather differently from the way they were designed to be connected. Buckminster Fuller devised these components to build omnitriangulated geodesic shells, polyhedra, and related structures (e.g., the icosadeltahedra in Fig. 6). Geodestix toy sets consist of: rigid sticks that can serve as polyhedron edges; and flexible plastic connectors that can join from three to eight sticks to form a polyhedral vertex. Since the connectors are flexible, triangles are the only stable polygons that can be built, and these components are ideally suited for building polyhedra with triangular faces (deltahedra). But beyond this, the simple, versatile plastic connector with its flexibly joined arm sockets radially arrayed around the orthogonal central hole provides a high degree of built-in adaptability for other construction purposes. I had been using Geodestix components to construct icosadeltahedra to illustrate the surface lattice designs (Fig. 6) and the next step was to find ways to build models representing the structure of virus capsids. The assembled model in Fig. 4 was the culmination of this search. Earlier versions, built with ping pong balls, poppet beads, or rubber stoppers, illustrated the morphological appearance of hexamer and pentamer "capsomeres." Arrangements of bits of rubber tubing attached to icosahedral cores showed how the morphology seen in electron micrographs could arise from clustering of identical structural units. Assemblies of tapered cardboard prisms held together by paper clips (similar to the model shown in Fig. 8 a) represented assembly of identical structure units without an underlying core, but the structure of these models did not appear to arise naturally from the bonding of the structure units. An idea for an adaptable model illustrating quasi-equivalent bonding of identical units was based on Fuller's "tensegrity" principle using his Geodestix connectors in a novel way. This provided the foundation for the self-assembly model in Fig. 4.



## TENSEGRITY

Fuller has developed a variety of discontinuous-compression, continuous-tension structures patterned such that individual struts do not touch, yet hold the tension network outwardly firm (Marks, 1960). He coined the word “tensegrity” to describe these structures, since their stability is due to their “tensional integrity.” A local stress applied to a tensegrity structure is distributed by the tension members to resist deformation. The extent to which such a structure can be deformed is determined by the elasticity of the tension members and the flexibility of the compression members. When the stress is removed the structure will return to the original equilibrium state if there has been no plastic deformation.

Fuller and his students have built icosahedral tensegrity shells from identical compression members held together by adjustable length tension members. It appeared that such structures might be built with both identical compression and identical tension members if the tension members could be deformed to accommodate the quasi-equivalent connection. I realized a solution to this design problem by adapting the Geodestix connectors as deformable links in a tensegrity structure built from identical units. Since the designs of the icosahedral surface lattices are derived from folding up the plane hexagonal net, the first step for constructing a dynamic shell model was to make a plane hexagonal tensegrity net. All the contacts between any structure unit and its neighbors in a plane hexagonal lattice can be resolved into three classes: those that lead to connection of the subunits into hexamers, trimers, and dimers. Any two of these three classes are sufficient to build a coherent hexagonal network. A simple model for a structure unit designed to build a plane hexagonal lattice can be represented by a stick with two attached flexible arm sockets that can connect to the ends of two neighboring sticks, as shown in Fig. 5 *a*. One end of the stick and its complementary socket form a trimer connection, and the other end of the stick and its complementary socket make a hexamer connection. This representation of the structure is quite general, since any structure unit can be mapped uniquely onto this model.

The stick and two-arm connector unit is the basic linking part of the assymetric structure unit shown in Fig. 3. For any asymmetric object a top and bottom, front and back, left and right can be defined as indicated in Fig. 3. The same anatomical features could be defined for

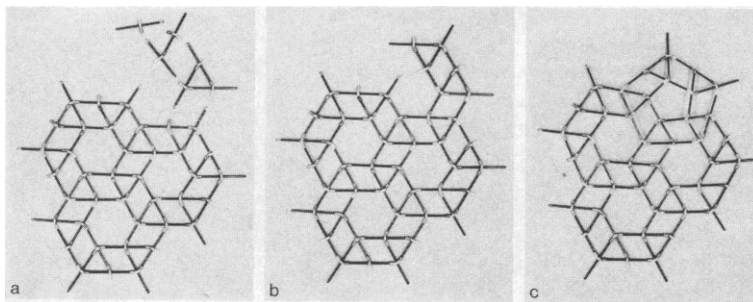


**Figure 5** Tensegrity nets. (*a*) Plane hexagonal net with, upper right, a single structure unit (consisting of a stick and two-arm connector), a pair of units connected by a trimer bond, and a trimer. Considering the two ends of the stick and the two arm sockets to be coded the same as the asymmetric unit in Fig. 3, the trimer bonds are between what is defined as the front end of the stick and the right arm socket, and the hexamer bonds are between the back end of the stick and left arm socket. (*b*) The unassembled units in *a* added to the hexagonal net. (*c*) A pentamer has been formed using “hexamer” bonds. The “tension” parts of the structure unit connecting the arm sockets to the sticks have been distorted and the net is now curved. The bonds are still the same as in *a* and *b* but the conformation of the units are now quasi-equivalent.

the stick and two-arm connector unit of Fig. 5 *a* by appropriate color coding as for the components of the Kabul dome. The difference here is that all the units are the same. Assembly of these units following exactly the same bonding rules for each unit must necessarily lead to a plane hexagonal net. Fig. 5 *b* shows the incorporation of the unassembled units in Fig. 5 *a* into part of the hexagonal lattice. The plane hexagonal net can be transformed into a convex surface by using hexamer bond sites to form pentamers. The tensegrity net with one pentamer formed is shown in Fig. 5 *c*. The physical connections between the sticks and sockets are still the same as in Fig. 5 *b*, but they are no longer geometrically equivalent. The links between the two arm socket domains and the stick domains of each structure unit are stretched and twisted when the units are connected to form a pentamer. If the arms could only pivot relative to the sticks, then the trimer would be rigid and only a regular plane hexagonal net could be formed. This adaptability of the Geodestix connectors is an unplanned, anticipatory feature of Fuller's design that is analogous to the unplanned but purposeful adaptability intrinsic to living structures.

Introducing pentamers as in Fig. 5 *c* produces a doubly curved surface. To form a closed shell, 12 and only 12 pentamers are topologically required. The most stable closed shells are those with icosahedral symmetry. Fig. 6 shows the first four icosahedral tensegrity shells corresponding to the icosahedral surface lattices with triangulation numbers  $T = 1, 3, 4, 7$ . There is no built-in curvature in these models; the same units can build shells of any triangulation number since the bonding is confined to a single surface. Built-in curvature defined by bonding interactions at different levels in a structure unit with radial extent, such as that illustrated in Figs. 3 and 4, naturally determines the triangulation number of the icosahedral shell that the structure unit can form.

#### MOVEMENT IN ICOSAHEDRAL SHELLS

Tensegrity models illustrate simply the distribution of energy in the surface that is determined by the mechanical properties of the structure units. The shape, which is between a sphere and

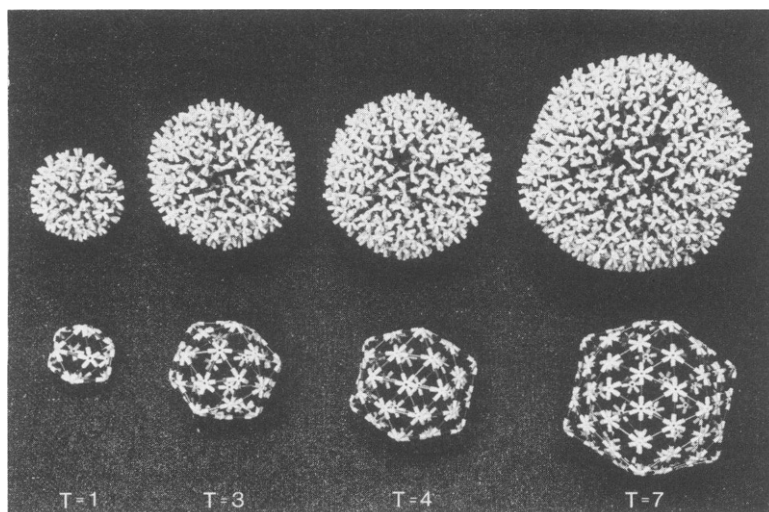


**Figure 6** Icosahedral tensegrity shells (top) corresponding to the icosahedral surface lattices represented by icosahedra (bottom) with triangulation numbers  $T = 1, 3, 4, 7$ . Each tensegrity shell is built of 60  $T$  structure units consisting of a stick and a six-arm connector; but only two arm sockets are used for bonding following the pattern in Fig. 5.

an icosahedron, is determined by this energy distribution. The shell will deform in response to externally applied stress but springs back to its original shape when the stress is removed. With age, however, the connectors of the  $T = 3$  shell, shown in Fig. 7, have slipped and plastically deformed under the action of gravity. The response of three young  $T = 3$  dynamic models to imposed stress is shown in Fig. 8. It is evident looking at these pictures that an icosahedral pattern of connection does not insure that the shell will have geometrically regular icosahedral symmetry. At the molecular level thermal fluctuations can produce variations in the shape of icosahedral virus capsids commensurate with the intrinsic flexibility of the structure.

These models might seem somewhat removed from reality considering the perfection evident in the structure of crystalline viruses. The structure of tomato bushy stunt virus (TBSV) has now been brilliantly revealed at a resolution of 2.9 Å by the crystallographic studies of Harrison and his colleagues (Harrison et al., 1978); and a similar picture of the molecular structure of southern bean mosaic virus (SBMV) is emerging with comparable clarity from the studies of Rossmann and his colleagues (Suck et al., 1978). These crystalline viruses have been selected for detailed structural studies because, under the conditions that the crystals are grown, the virus particles have rigid, highly symmetric structures. These same viruses can, however, be swollen by removing bound divalent cations at slightly alkaline pH following procedures worked out in some detail for SBMV (Hsu et al., 1976). Structural studies on crystals of the swollen virus particles are limited by the disorder in the crystals (Rayment et al., 1979). Small angle diffraction measurements from solutions and microcrystals of swollen SBMV show that there is substantial variation in the shape of the particles. The positions of the subunits in the capsid vary relative to the particle center with a standard deviation of ~6 Å (Li, Fricks, D. L. D. Caspar, and Rayment. Manuscript in preparation). This disordered structure can be switched back to the highly ordered compact form by adding back divalent cations. NMR spectra from the compact and swollen form indicate that the disorder on swelling is dynamic. Movement in the swollen virus particles is a nuisance for the crystallographer trying to solve its structure, but this flexible structure may be closer to the more active state of the virus particle during its assembly or disassembly. In the compact form of the virus structure, the intrinsically flexible subunit is locked into the distinctly different but quasi-equivalently related conformations revealed by the high resolution x-ray crystallographic analysis (Harrison et al., 1978).

A very simple model illustrating rigidity in a  $T = 3$  icosahedral lattice is shown in Fig. 9. This model is built of 90 identical pieces of sheet aluminum bent to represent a dimer pair. This was the last of the icosahedral models built by the late Charles Ingersoll, Sr.; he had the pieces sheared and bent with equipment at the Boston Navy Yard since we lacked the technology for such sheet metal work at The Children's Cancer Research Foundation. The adjustments required in the model units to fit into the three quasi-equivalently related environments are accommodated by a  $\pm 2.2^\circ$  change in the dihedral angle of the metal dimer and the very small movement allowed by the slots where pieces are held together by the machine screws. Small changes in the "bonds" holding this structure together lead to larger differences in the subunit arrangement. By mutual support the quasi-equivalently bonded, identical, but moderately deformable, thin-sheet subunits form a strong and stable assembly.

#### PERIODICALLY PERTURBED DAHLEMENSE HELIX

Before the concept of quasi-equivalence was formulated, the one experimentally recognized example of this phenomenon in protein packing was the periodic perturbation of the subunit

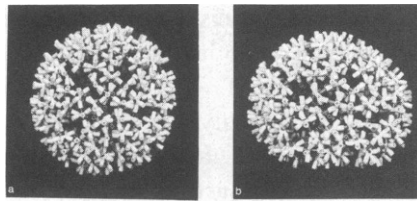


Figure 7 On the left (a)  $T = 3$  tensegrity shell from Fig. 6 (1962 photograph). On the right (b) the same model, after sitting on the shelf for 18 years has sagged and developed a flat bottom.

structure in the dahlmense strain of TMV (Caspar, 1963). Dahlemense x-ray diffraction patterns that K.C. Holmes and I obtained in 1960 had presented a puzzle: meridional reflections, “forbidden” from any regular helix, were observed on layer-lines with twice the helix pitch spacing. Carolyn Cohen saw an analogy with the  $\alpha$ -helical “coiled-coil” diffraction pattern (Crick, 1953) that provided us with the clue to solve the puzzle (Caspar and Holmes, 1969). These forbidden reflections are like the Rowland ghost spectra that arise from periodic

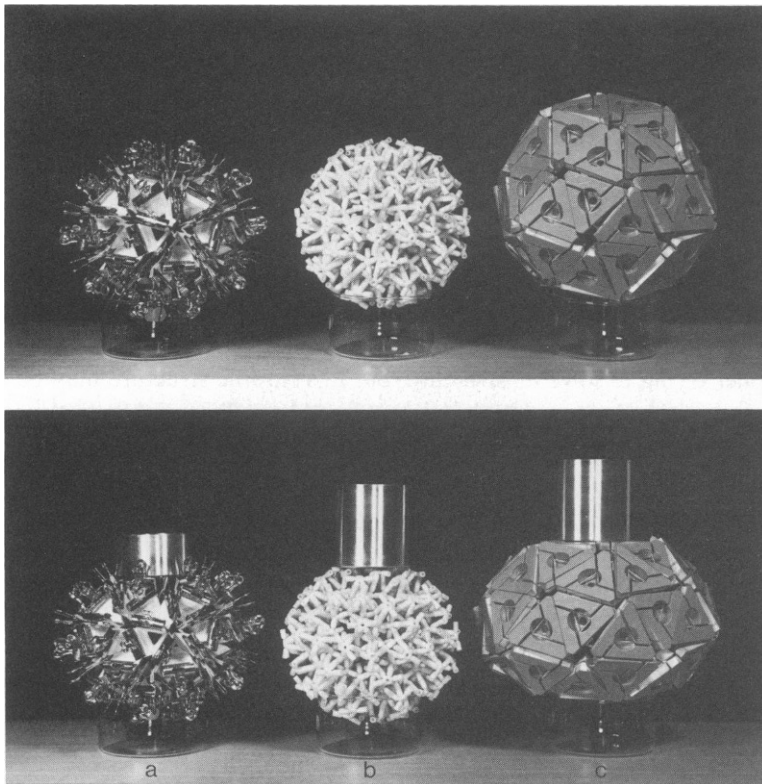


Figure 8 The effect of stress on 3 dynamic  $T = 3$  models. To set the scale, the model in the center is 5 in. in diameter and the two larger weights weigh two lb and the two smaller one lb. (a) Model made of 60 cardboard trimers in the form of truncated pyramids with flaps held together with spring clips making dimer connections. The model is somewhat floppy and sags under its own weight. Adding one lb weight in the lower picture only slightly increases the flattening. (b) Tensegrity model as in Fig. 6 with 90 additional connectors in twofold positions cross-strutting the underlying network. This model performs only slightly under a two lb weight. (c) Model made of rigid wooden trimers connected by dimer bonds form by rubberbands. Unstressed, the rubber bands maintain a symmetric shape, but the two lb weight in the lower picture flattens the model to about  $3/4$  of its unstressed thickness.

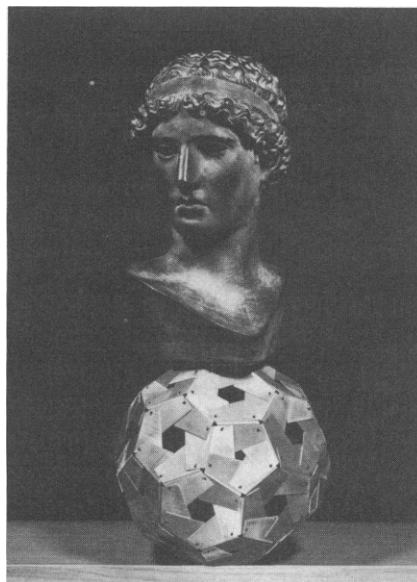


Figure 9 Rigid T = 3 model made of 1/32 in. thick sheet aluminum dimers connected by pentamer/hexamers. The diameter along the threefold axis is 11.5 in. and the model weighs two lb. Its shape is approximately that of a truncated Platonic icosahedron and, without distortion, it supports a 32 lb plaster Platonic head.

errors in the ruling of optical diffraction gratings. The perturbation, which involves small up and down displacements of the outer end of the subunits, repeats exactly after two turns; since the virus helix has an integral number of units in almost exactly three turns, the periodically perturbed structure repeats in six turns. In this distance there are 98 subunits, each with a slightly different conformation.

The nature of the perturbation is illustrated in the drawings in Fig. 10, which compare the appearance of the common and dahlmense strains. As indicated more schematically in Fig. 11, the axial displacements arise from bending of the outer ends of the protein subunits at hinge points located at  $\sim 70$  Å radius. The  $\pm 3.5$ -Å maximum axial displacement of the outer end of the subunit at  $\sim 90$  Å radius corresponds to a bending at the hinge of  $\pm 10^\circ$ . Bending may not be localized all at one point but may be distributed over some segment in the molecule. The line of maximum axial displacement is exactly parallel to the helix axis, and the magnitude of displacement changes very smoothly from one unit to the next along the outside edge of the helix. However, the mean length of the regularly perturbed domains is only about one-sixth the length of the particle.

Energy for the periodic deformation must be provided by axial interactions between the outside ends of the subunits. To make these bonds, identical parts of neighboring molecules must be brought closer together than the pitch of the helix determined by the close packing of the subunits at a smaller radius: thus, there is no strictly regular way in which all these bonds can be formed. Since the deformed structure is stable, the decrease in free energy on forming some of the possible additional bonds is greater than the increase in free energy required to move the subunits into the 98 slightly different but quasi-equivalent positions. The relative axial displacement of neighboring units along the helix changes very smoothly; thus, this perturbation produces a minimal stretching of the side-to-side bonds. That the movements of the outside ends can be represented by a smooth sinusoidal axial displacement which repeats

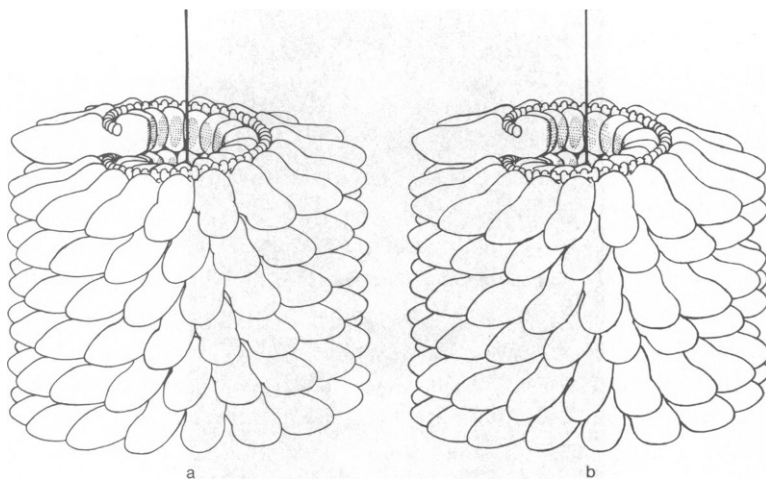


Figure 10 Comparison of 6-turn helix segments of (a) common strain and (b) the dahlemense strain of tobacco mosaic virus, (Caspar and Holmes, 1962). In the common strain the subunits are equivalently related and the outer ends of the subunits are not in contact with the axial direction. In the dahlemense strain, turns of the helix on the right side are alternately in contact and displaced from each other. The net result of this periodic distortion is that the subunits occur in 98 symmetrically distinct but quasi-equivalent conformations.

exactly after two turns implies that the perturbation results from nonlinear axial forces drawing the ends of subunits in neighboring turns closer together, while, simultaneously, the perturbation is constrained by a strong side-to-side bonding interaction that is relatively undeformable.

#### MOVEMENT IN THE DAHLEMENSE HELIX

There is no physical requirement that the line of maximum axial displacement (shown on the right side of the helices in Figs. 10 and 11 remain fixed on one side of the particle. As this line is rotated about the axis it passes through 98 equivalent positions that represent states of

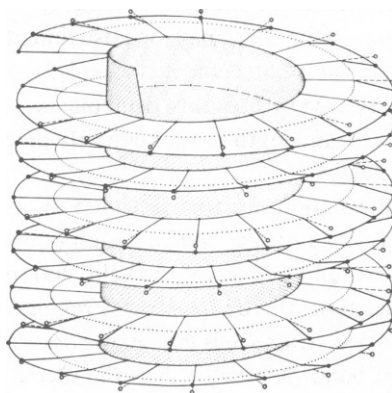


Figure 11 Schematic illustration of periodic distortion in the dahlemense helix. The subunits bend at a hinge point at about 70 Å radius with a  $\pm 3.5$  Å displacement of the outer ends at 90 Å radius. The perturbation is attributed to axial attractive interactions and is constrained by the relatively undeformable side-to-side bonding.

equivalent free energy (neglecting end effects). Since the activation energy for rotation of the line of maximum displacement around the particle axis may not be large, this line may sporadically rotate in one direction or the other under the influence of thermal fluctuations.

Considering the regularity of the deformation of the dahlemense helix, it is at first sight surprising that the length of the ordered domains is significantly less than the particle length. Since the periodic deformation is energetically favored, introducing any dislocations will lead to an increase in free energy of the intersubunit bonding. Limitation in the length of the regularly perturbed domains may be due to the increase in the rotational and translation entropy associated with an increased number of independent domains. The total configurational entropy per particle should increase as the number of domains increases in proportion to the logarithm of the number of additional configurations. Since the free energy of bonding increases linearly with the number of dislocations while the decrease in free energy from the configurational entropy is less rapid, there will be some number of dislocations at which the free energy per particle is a minimum. The experimentally measured length of the regularly perturbed domains corresponds to a mean of about five dislocations per particle. Although the structure is highly ordered, there appear to be coordinated internal motions which involve small changes in the conformation of the subunits. Flexibility of the protein subunit as seen in the dahlemense helix appears to be an essential property for the self-control of the assembly process in all strains of TMV.

#### $\alpha$ -HELICAL COILED-COIL

Quasi-equivalent bonding as observed in the dahlemense helix is more likely to be the rule, rather than the exception, in ordered structures built of protein molecules. With molecules as complicated as proteins it is unlikely that all the energetically favorable interactions between pairs of units in an assembly will be compatible with a symmetrically regular arrangement in which identical units are strictly equivalently related. If deforming the bonds or the molecules in some systematic way leads to the formation of more stable bonds than regular packing, then identical units will be quasi-equivalently related in an ordered structure. This is what happens on a smaller scale in the two or three chain  $\alpha$ -helical coiled-coil structures (Crick, 1953; Pauling and Corey, 1953). Starting with a straight  $\alpha$ -helix in which all peptide groups are equivalently related, these groups end up in seven distinct environments when the helix is supercoiled. The overall symmetry of the polypeptide chain backbone can be represented by equivalently related segments of seven peptides; however, since the departures from the regular  $\alpha$ -helix are small, all the peptide groups are quasi-equivalently related. The coiled-coil structure is very stable, since the increase in free energy required to periodically deform the regular  $\alpha$ -helix is more than offset by the decrease in free energy resulting from the interlocking of nonpolar side-chain groups (Cohen and Holmes, 1963; McLachlan and Stewart, 1975).

#### ICE

Having formulated the concept of quasi-equivalence to understand the intricate structures formed by protein molecules, it became evident that the same idea describes structural relations that occur in crystals of very simple molecules. Water molecules form a variety of ordered structures. There are nine polymorphs of ice (Kamb, 1965) and a number of clathrate hydrates in which shells of water molecules (reminiscent of the icosahedral virus capsids) contain "guest molecules" in their cavities (Pauling, 1960). In all forms the water

molecules are tetrahedrally hydrogen bonded, but the hydrogen bonds are only arranged with perfect tetrahedral symmetry in the metastable low pressure cubic ice polymorph Ic and in the high pressure ice VII. Nearly perfect tetrahedral coordinate occurs in ice I, the familiar hexagonal form; there are, however, two symmetrically distinct but quasi-equivalent hydrogen bonds: three of one type related by a threefold axis, and one of the other type along the threefold axis. The bonds in some of the high pressure polymorphs occur in several different distinct conformations which allow denser packing. Distortion of the hydrogen bonds in ice II and ice V, for example, into eight quasi-equivalent conformations with higher energy than the two almost equivalent bonds of ice I, leads to lower energy structures at high pressure because of closer packing. Thus, even with very simple molecules quasi-equivalent bonding can lead to stable structures, although more symmetric crystalline arrangements are physically possible.

## CRYSTALLIZATION AND NUCLEATION

Analogies with crystallization spring to mind when considering the problem of biological assembly. Self-assembly, when first conceived (Caspar and Klug, 1962), was considered to be a process akin to crystallization. It is in the transition from a state in which the subunits are randomly arranged to a state in which they are highly ordered that virus assembly appears to be like crystallization. The driving energy for formation of the ordered structures is provided by the "bonds" between the units. Association of the parts can proceed without an external source of energy or a master template. The order in the final structure is a necessary consequence of the statistical mechanical compulsion to form the maximum number of most stable bonds between the units. Self-assembly is unlike crystallization, however, in that the biological process is purposefully controlled. Initiation is the beginning of this purposeful process.

Crane (1950) recognized that biological growth is a "nonself-starting" process. Although he was considering principally what we know today as template controlled synthesis, what he illustrated was how nucleation could be applied to regulate the initiation of a subunit assembly process. Nucleation is, in fact, essential for the formation of any structure in which each unit bonds with more than two nearest neighbors. This is the case for ordinary crystallization in which monomers in solution are in equilibrium with crystals. Molecules at a boundary with some bond sites unoccupied are in a higher energy state than those whose bonding potential is saturated within the aggregate. The initial stage of growth under these conditions is highly unstable; only when such an aggregate exceeds some critical size is further growth spontaneous. Crystallization is usually initiated by some adventitious nucleation process which holds enough molecules together to get the spontaneous association started.

Oosawa and Kasai (1962) formulated a theory for assembly of units in a helix which took into account the fact that the equilibrium constant for adding units to form the initiating nucleus will generally be less than the equilibrium constant for continued addition to the helical structure. The simple geometrical explanation of this behavior is that more stabilizing bonds can be formed by adding a unit to the growing helix than to the incomplete first turn. In the growing helix, the unit being added forms bonds with the previous unit at the end of the helix as well as with one or two units in the turn below. If the energy associated with the different bonds is comparable (and if this energy is independent of the size of the aggregates), the free energy for adding to the growing helix could be two or three times that for adding a unit before the first turn is complete. When there are only a small number of units in the first stable aggregate and when the bond energy is moderate (as is the case for small aggregates of TMV protein (Caspar, 1963; Durham and Klug, 1971)), then the polymerization process will



not appear very cooperative. Oosawa and Kasai's theory includes an adjustable parameter that can represent a situation in which the formation of the initiating nucleus is very improbable even when the geometric considerations would suggest a more moderate difference between the equilibrium constant for initiation and that for growth. We can see now that such control can be provided by a molecular switching mechanism homologous to allosteric regulation (Monod et al., 1965).

### BACTERIAL FLAGELLA ASSEMBLY

Asakura (1968) has shown that the assembly of bacterial flagella, which in some ways resembles crystal growth, differs from crystallization in the fundamental nature of the rate limiting process. In fact, a homology may exist between flagellin polymerization and allosteric switching. Solutions of flagellin monomers will associate in vitro if seeds of fragmented flagella are added but otherwise will remain dissociated (Asakura et al., 1964). Unlike seeded crystal growth where the rate of addition depends principally on collision frequency, once the critical size aggregate is exceeded, Asakura showed that the rate of growth of the flagellum is limited by the time it takes for the monomer to change its conformation to the polymer form at the site of attachment. The growing flagellum acts like a catalyst to change the conformation of bound monomer. As a monomer is incorporated at the end of the filament, it is converted to the state that has high affinity for like units in the polymer; in this associable state the monomer can act to catalyze the incorporation and conversion of the next unit, and so on and so on. The rate of polymerization measured as a function of monomer concentration follows Michaelis-Menton kinetics: like an enzyme reaction the rate approaches a limiting value at high monomer (e.g., substrate) concentration, and the ratio of this limiting rate to the seed (e.g., enzyme) concentration is a constant. The conformational switching of the flagellin unit differs from that of an allosteric enzyme in that flagellin acts as its own allosteric effector. It is the binding of monomer to the growing filament that triggers the conformational change of the monomer to the high affinity, associable state.

Self-control of flagella assembly as demonstrated by Asakura's studies on solutions of pure flagellin illustrates the same general principle deduced by King and his colleagues (King and Mykolajewycz, 1973; Kikuchi and King, 1975) on the more complex pathway of bacteriophage T4 tail assembly: protein molecules destined to build larger structures appear to be synthesized in a state in which they do not spontaneously assemble; rather, they are activated by interaction with, and incorporation into, the growing structure. Thus, the regulation of the assembly pathway takes place at the level of the assembly process itself by limiting reactive sites to growing structures. Switching of an inactive structural protein to an active, associable conformation by interaction with the assembly it is destined to join could be called autosteric by homology with allosteric switching.

### ACTIN ASSEMBLY

Conformational switching appears also to be involved in the polymerization of G-actin to form F-actin. The concentration dependence of the polymerization can be accurately represented by the thermodynamic model of Oosawa and Kasai (1962) with a very small equilibrium constant for initiation and a much larger one for growth. From careful measurements of the polymerization (at 20 in  $10^{-3}$  M  $\text{CaCl}_2$ ,  $5 \times 10^{-4}$  M ATP, pH 7.5) as a function of actin concentration and time, Wegner and Engel (1975) determined that the equilibrium constant,  $K$ , for adding monomer to the growing filament is  $1.7 \times 10^5 \text{ M}^{-1}$  corresponding to a free

energy change of  $-7.2$  kcal. However, the equilibrium constant for forming the dimer (which is the critical nucleus for further growth) is  $4 \times 10^{-2} \text{ M}^{-1}$ , corresponding to a free energy change of  $+2.0$  kcal. Since the free energy for formation of dimer is  $+9.2$  kcal greater than the free energy change for adding a unit to the growing polymer, no detectable polymerization is observed until the monomer concentration reaches the critical value of  $1/K = 5.9 \times 10^{-6} \text{ M}$  (where  $K$  is the equilibrium constant for monomer addition to the polymer). Thus, actin polymerization has the cooperative appearance of a crystal phase transition that can be described by Gibbs' phase rule. Cooperativity in crystal growth results because many units must be combined in a crystal nucleus before spontaneous growth will proceed. The appearance of cooperativity in the actin polymerization is due, however, to the energy barrier that has to be overcome to form the initiating dimer. To account for this energy difference Wegner and Engel (1975) suggested a model in which the initiating dimer is weakly bonded because of a bad contact, but the addition of a third unit transforms the bad contact into a stable one.

From critical analysis of the kinetics of actin polymerization, Wegner (1976) has established that the process is remarkably dynamic in the presence of ATP: the filaments grow at one end while shortening at the other. Under steady-state conditions a unit added at the growing end will sometime later dissociate from the other end, having moved the length of polymer. Dephosphorylation of ATP makes the effective equilibrium constant at the growing end different from that at the other end of the filament. If there were no source of energy, reversibility would require the same equilibrium constant at the two ends. Growth may, nevertheless, be unidirectional in a reversible association process since the rate constants need not be the same at both ends; however, directed motion as in the movement of actin units through a fixed length filament requires a source of energy. The difference in association constant at the two ends implies a difference in structure that is linked to the hydrolysis of ATP. It is difficult to imagine any way in which the structures at the two ends could be directly visualized. Could there be a gradient of quasi-equivalently related conformations along the length of the dynamic F-actin filament?

#### AUTOSTERY AND ASSEMBLY

Flagellin polymerization, the G to F transformation of actin,<sup>4</sup> formation of the tail of bacteriophage T4, and the self-assembly processes of other proteins have the common property recognized by King that protein molecules destined to build larger structures are made in a form in which they do not spontaneously associate. Self-controlled conformational switching is the essence of the regulatory mechanism. This kind of autosteric control for initiating assembly is entirely different from the nucleating mechanism involved in crystal growth.

Crystallization does not require conformation switching. The nature of the bonds between molecules in a crystal, and the energy associated with these bonds, can be presumed to be independent of the size of the crystal. As the crystal grows, the mean number of bonds per molecule increases approaching the number formed by a molecule inside the crystal. For example, in a simple cubic crystal of  $n^3$  molecules, where  $n$  is the number on a side, the ratio of bonds to molecules is  $6(1 - 1/n)$ , which is very close to 6 if  $n$  is large. For a very small crystal, say one made of eight molecules, the number of bonds per unit is only half that of a large crystal, and, correspondingly, the mean bond energy per unit is half that of the large crystal. Thus, in a saturated solution, small crystals, below some limiting size, are always less stable

than smaller crystals, and so on, down to the monomer whose concentration is greater than that of any small aggregate. Nucleation for crystal growth is basically the geometric problem of getting it all together: a relatively large number of molecules must form an arrangement that has a very low probability of occurrence before spontaneous growth can proceed.

Autosteric switching in protein association can give the appearance of a highly cooperative process even for formation of a one-dimensionally periodic structure, which, thermodynamically, is never supposed to undergo a phase transition. The free energy of the polymer can be factored into two terms: "bond" energy  $\Delta G_b$  and "conformational" energy  $\Delta G_c$ . Bond energy is the change in free energy on adding a monomer to the polymer in the high affinity, associable state. Conformational energy is the difference in free energy between the monomer in its associable state and the monomer in its low affinity, unsociable state. The change in free energy  $\Delta G_c$  in switching from the unsociable to associable conformation must be positive, for otherwise the monomers would already have formed polymers. The change in free energy  $\Delta G_b$  on forming a bond in the polymer in the associable state must be negative or the polymer would never form. Assuming that all the bonds in the linear polymer are the same, independent of size, the free energy change for forming a dimer in the high affinity state from two monomers in the low affinity state is:  $\Delta G_2 = \Delta G_b + 2\Delta G_c$ ; on adding a monomer to the growing polymer, which entails switching the monomer from the unsociable to associable conformation and forming one high affinity bond, the free energy change is  $\Delta G_a = \Delta G_b + \Delta G_c$  (this net free energy change is assumed to be independent of size, neglecting the weak dependence of the configurational entropy of the polymer on its size). If the polymer is to form,  $\Delta G_a$  must be negative but  $\Delta G_2$  may be positive. Under these circumstances the monomer-polymer transition will appear to be highly cooperative, like actin polymerization.

#### ACTIN AUTOSTERY

For actin, each unit added to the dimer or any larger aggregate will bond with the two previous units forming two "bonds", whereas there is only one "bond" for the dimer. If  $\Delta G_b$  is the dimer bond energy, then the bond energy for addition to larger polymers will be  $r\Delta G_b$ , where  $r$  is the ratio of the bond energy for addition of a unit to the larger aggregate compared to that for forming the dimer. By extension of the analysis for the one-dimensional polymer to the actin helix,  $\Delta G_a = r\Delta G_b + \Delta G_c$  and  $\Delta G_2 = \Delta G_b + 2\Delta G_c$ . The ratio  $r$  cannot be greater than 2: if one bond is stronger than the other, most of the dimers will be connected by the stronger bond, all units, of course, being in the high affinity state. Taking  $r = 2$ , and the free energy changes  $\Delta G_a = -7.2$  kcal and  $\Delta G_2 = +2$  kcal as measured by Wegner and Engel (1975) for actin, then the mean free energy change for forming one bond in the associable state is  $\Delta G_b = -5.47$  kcal, and the free energy change for switching from the unsociable to the associable state is  $\Delta G_c = +3.73$  kcal. Taking  $r = 1$ , which corresponds to a simple one dimensional polymer with no nucleation effect, then  $\Delta G_b = -16.4$  kcal and  $\Delta G_c = +9.2$  kcal; in this case the conformational energy term would account for all the difference between the free energy for dimer formation and that for polymer growth. Since  $1 \leq r \leq 2$ ,  $+3.7 \leq \Delta G_c \leq +9.2$  kcal; thus, the difference in conformational energy between the unsociable and associable form of the monomer accounts for a substantial part of the energy barrier for initiating polymerization.

Representation of actin self-assembly as a two-state autosteric transition with the polymer acting as the autosteric effector may be an oversimplification, since the role of ATP binding and dephosphorylation has been overlooked. Monomeric actin, which is presumed to be

predominantly in the unsociable form, has high affinity for ATP, whereas filamentous actin, which is defined as the associable form, has ADP bound. Nucleotide splitting is not, however, necessary for filament formation, since monomeric actin with ADP bound still polymerizes, but at a slower rate than with ATP (Hayashi and Rosenbluth, 1960); furthermore, polymerization also occurs when the nucleotide is replaced by an ATP analogue which cannot be dephosphorylated by actin (Cooke and Murdoch, 1973; Mannherz et al., 1975). The measurements of the equilibria in actin polymerization by Wegner and Engel (1975) have all been made in the presence of sufficient ATP to saturate the monomeric actin. Splitting of ATP drives the flow-through, head-to-tail polymerization of actin (Wegner, 1976); and ATP could also act as an allosteric effector in stabilizing the unsociable, monomeric form, or perhaps some third state of actin. Nevertheless, Wegner and Engel's (1975) measurements can be described by a simple equilibrium model and a significant part of the energy barrier for initiation of polymerization can be accounted for by a simple autosteric switching mechanism. Autosteric switching between an unsociable and associable form of a structural protein appears to be a basic self-control mechanism in self-assembly. Description of actin assembly in these terms simply illustrates the principle.

### TMV PROTEIN ASSEMBLY

Literally and figuratively, TMV is where the self-assembly story started when active virus was first reconstituted from its protein and nucleic acid components by Fraenkel-Conrat and Williams (1955). The design for the virus structure is embodied in the protein subunits, since they can assemble themselves into the same helical structure as in the complete virus without the RNA chain (Franklin, 1955). Association of TMV protein is a step-wise process that proceeds through stable intermediates of increasing size. Stability of these intermediates implies that the bonds in small aggregates are stronger than in larger aggregates (Caspar, 1963). If the bonding were the same in aggregates of different size, as in ordinary crystals, then once association started it would proceed to the aggregates of largest size. Both autostery and quasi-equivalence are involved in self-control of TMV protein assembly. Since the favored bonding in small aggregates cannot continue in larger aggregates, the units in the smaller aggregate must be quasi-equivalently related: adding another unit produces a smaller decrease in free energy than adding the previous one. Transitions to larger aggregates must involve autosteric switching to a conformation in which the mean energy per bond is weaker than in the smaller aggregates but in which the ratio of the number of bonds to the number of subunits is larger. To describe the equilibria among the TMV protein aggregates I factored the free energy change for forming an  $n$ -mer into a "bond" energy term and a "distortion" energy term. The distortion energy term represents the energy required to switch a subunit into a conformation in which it can associate in a larger aggregate. Both conformational and geometric factors are significant in the switching among the different states of association. My predictions about the stable intermediate states of TMV protein assemblies based on the presumption that the nearest neighbor packing relations of subunits in smaller aggregates would be similar to that in the completed helix are now largely confirmed (Durham and Klug, 1971; Vogel et al., 1979). A half-dozen or so distinct but closely related conformational states corresponding to different stable intermediates may be necessary to adequately describe the TMV protein association. The complexity of this self-nucleated and self-controlled assembly process may extend indefinitely the richly rewarding experimental studies relating the structures and forces involved in the generation of this simple virus particle.

## SWITCHING FROM DISK TO HELIX

Assembly of the TMV particles is nucleated by the interaction of two turn protein disks (Butler and Klug, 1971) with a specific hairpin loop of the viral RNA (Lebeurier et al., 1977; Butler et al., 1977). In this process the disk is switched into a two turn helix segment. Comparison of the electron density map of the protein disk crystal (Champness et al., 1976) with that of the virus (Holmes et al., 1975) showed that the polypeptide chain conformation is similar in the two states, but the axial bonds connecting the two rings of the disk are substantially different from the axial bonds linking successive turns of the virus helix. (These differences are larger than I had anticipated in my prediction of the disk-helix relation). Possible pathways for switching can be inferred by trying to identify the connections that are conserved in the structural transition. The problem is analogous to the prediction of possible pathways for bacteriophage tail sheath contraction, from comparison of the extended and contracted structures. Moody (1973) determined the contraction mechanism from electron micrographs of partially contracted sheaths. This sort of information about the structure of intermediate states, which is necessary for mapping the switching mechanism, is lacking for TMV. In the switching from disk to helix there must be an axial displacement at a dislocation coupled with rotation of the top layer relative to the bottom. There are two ways in which this rotation can occur: by about half the side-to-side separation of the units either to the right or the left. The right twist will produce a helix segment with  $16 \frac{1}{3}$  units per turn and the left twist would give a helix with  $17 \frac{1}{3}$  units per turn. The association of protein disks with RNA to form virus particles generates a helix with  $16 \frac{1}{3}$  units per turn. Repolymerization of the protein alone, however, produces helices with either  $16 \frac{1}{3}$  or  $17 \frac{1}{3}$  units per turn (Mandelkow et al., 1976). That the  $17 \frac{1}{3}$  units per turn helix does exist suggests that it may play some role during assembly, but without a realistic picture of the sequence of events in the virus assembly, all mechanistic models are fanciful. There are no evident prospects of actually visualizing the switching process, but by comparison of the structure of polymorphic forms and by relating the kinetics of their formation it may be possible to define the critical steps on the assembly pathway.

## BACTERIOPHAGE T4 TAIL ASSEMBLY

The assembly pathways of bacteriophage T4 have been mapped in rich detail from studies on the structures in cells infected with conditional lethal mutants (Casjens and King, 1975). There are three independent subassembly pathways for the formation of the head, tail, and tail fibers. A common feature to the regulation of the assembly of these different structures is that the products of the genes function in an orderly sequence which is defined by the gene product interaction rather than by sequential gene expression. T4 tail assembly as analyzed by King and his colleagues (King and Mykolajewycz, 1973; Kikuchi and King, 1975) clearly exemplifies control mechanisms that are generally significant for understanding morphogenesis. Tail formation requires at least 21 gene products and involves first, assembly of the hexagonal baseplate, and then polymerization of tube and sheath subunits on the baseplate, followed by termination of the completed tube and sheath.

In the absence of the completed baseplates the tube subunits have no tendency to aggregate in infected cells; but tube subunits purified from disrupted phage can be reassembled in vitro without baseplates into tubes of varying lengths (Poglazov and Nikolskaya, 1969). Sheath assembly is somewhat less tightly regulated than that of the tube, since the subunits will eventually polymerize into a contracted polysheath in cells infected with mutants that do not

produce a normal tail precursor structure. If the first proteins in tail assembly are missing due to mutation, then, except for the formation of some polysheath, all other tail proteins remain unassembled as free subunits.

Synthesis of T4 tail proteins in a form in which they do not spontaneously associate provides the essential basis for regulation of tail assembly (Casjen and King, 1975). Assembly is controlled through activation of the latent bonding potential of unreactive units by the assembly process itself. Generation of the appropriate combining sites in the reacting units is dependent upon correct completion of the previous steps in assembly and anticipates the next steps to be taken. This self-control mechanism may be fundamental in the morphogenesis of many biological structures. The same kind of autosteric switching to activate a latent bonding potential can be seen in the self-control of T4 tail sheath contraction and a similar sequential switching mechanism may operate to regulate the length of the tail tube assembly.

#### T4 TAIL SHEATH CONTRACTION

Moody's (1973) deduction of the contraction mechanism for the T4 tail sheath provides a structurally realistic picture of the self-controlled switching in this protein assembly. Characterization of a switching process starts with the determination of the initial and final structures; tracing the pathway for the change requires the identification of intermediate structures during the transition. Initial and final structures of some other important dynamic protein assemblies have been determined to much finer resolution than that of the T4 tail sheath, but Moody's analysis of the sheath contraction has led the way in demonstrating how to trace the pathway of purposeful movement in protein assemblies.

Contracted (Moody, 1967*a*) and extended (Moody, 1967*b*; Krimm and Anderson, 1967) T4 tail sheaths both are built of a helical arrangement of 24 annuli of 6 units each. In the extended structure the axial repeat distance is  $\sim 40$  Å and each annulus is rotated by  $\sim 17^\circ$  to the right relative to that below it; on contraction the axial repeat decreases to  $\sim 15$  Å, and the twist angle between an annulus and the one below is  $\sim 32^\circ$  to the right. The topology of the relation between the 144 sheath subunits is the same in both structures: The symmetry can be represented by a surface lattice consisting of 24 hexagonal rings connected by a set of six right-handed and a set of six left-handed helices. Moody (1967*b*) pointed out that this correspondence in symmetry means that the contraction can proceed by a displacive transition in which identical subunits behave the same way rather than by a reconstructive transition in which the topology of connection is altered.

The distinction between displacive and reconstructive transitions is fundamental for characterizing switching mechanisms. For example, conversion of the TMV protein disk to a helix segment is reconstructive at the dislocation, but the twisting of the two layers relative to each other that occurs in the disk-helix change (Champness et al., 1976) is displacive, since the topology of connection between layers is conserved. The activation energy for a reconstructive transition is likely to be large, since bonds must be broken and reformed with a different pattern of connection. Displacive transitions where there are only small relative motions of neighboring units, as in the allosteric switching from deoxy- to oxyhemoglobin (Perutz, 1970), can take place quite rapidly. The displacive transitions which are possible in the T4 tail sheath all involve large relative motions which may occur slowly, but in concert.

Contraction of the tail sheath proceeds by a 25 Å decrease in separation of annuli coupled with a rotation relative to each other. The smallest rotation that can produce the observed structural change is a twist to the right of  $15^\circ$  for each annulus relative to the one below it. However, since each annulus consists of six equivalently related units, a twist of  $15^\circ$  to the

right plus any multiple to  $60^\circ$  to the right or left would also produce the same final structure on contraction, e.g., a  $45^\circ$  twist to the left,  $75^\circ$  to the right, etc. The only convincing way to decide among these possibilities is to visualize the transitional structures.

Moody (1973) determined both the pathway for the contraction and the nature of the coupling from electron micrographs of tail sheaths trapped in the act of contracting. These transitional states were produced by treatment with alkaline formaldehyde; by varying the pH and time of treatment he was able to visualize different stages of the process. Contraction starts at the baseplate and proceeds as a wave up the sheath, generating transitional helical arrangements intermediate between the extended and contracted structure. From measurement of the twist angle for the transitional helices, he established that each annulus rotates  $15^\circ$  to the right relative to the one below during contraction. There is a sequential character to the switching, since contraction always proceeds from the base; but the long-range coupling is nevertheless fairly strong as stretches of the transitional helical structures were observed with a gentle gradient in the contraction. A gradient in the contraction suggests a continuous range of quasi-equivalently related conformations for the sheath subunits.

### DESIGN OF T4 TAIL SHEATH MODEL

The designing of a mechanical model for the contractile tail sheath (Caspar, 1976) began with the identification of conserved connections and variable linkages in the structure which could be conveniently represented by moving parts. Energy to drive the contraction was stored in springs which are stretched in the extended state. The objective of this sort of model building, as with the icosahedral virus models, is to represent the distribution of energy in the structure which determined the arrangement of matter. In the tail sheath model, however, the stored energy in the extended form must drive a purposeful change in structure.

The arrangement of sheath units can be represented by three unit vectors which define the surface lattice. The unit cells for the extended and contracted surface lattices are chosen to have some common features corresponding to nearest neighbor relations which are conserved on contraction. The vector between neighboring units in an annulus is one invariant: since the sixfold rotational symmetry is conserved on contraction this vector always subtends an angle of  $60^\circ$  from the axis. The two other vectors chosen to define the surface lattice are in the direction of the right- and left-handed set of six-start helices. The vector between lattice points of the extended structure which goes up  $40 \text{ \AA}$  and twists  $17^\circ$  to the right is transformed to the vector up  $15 \text{ \AA}$  and twisted  $32^\circ$  to the right in the contracted structure. At a radius of  $\sim 80 \text{ \AA}$  these vectors have the same length of  $\sim 47 \text{ \AA}$  in both structures, and the length of this connection is taken as another invariant for the model. The third link up to the left is variable, shortening on contraction from  $\sim 72 \text{ \AA}$  to  $42 \text{ \AA}$  at the  $80 \text{ \AA}$  radius.

### MECHANICS OF THE CONTRACTILE MODEL

Annuli of the sheath model (Fig. 12) constructed by Charles Ingersoll, Jr. are represented by 24 lucite rings which are connected by six flexible steel straps each fastened by 24 screws to represent the right-handed links with invariant length. The variable connections are made by steel coil springs connecting pairs of screws along the left-hand set of six-start helices. The scale of the model is  $1 \text{ in.} = 40 \text{ \AA}$ . Each spring exerts a pull of  $\sim 1 \text{ lb.}$  at the extended length for the 1 in. repeat spacing between rings (Fig. 12 a); the component of the pull along the axis is about half the spring tension, and this is counterbalanced in part by the compression of the steel strap helices. In Fig. 12 a Ingersoll is exerting a force of  $\sim 35\text{--}40 \text{ lbs}$  to extend the model

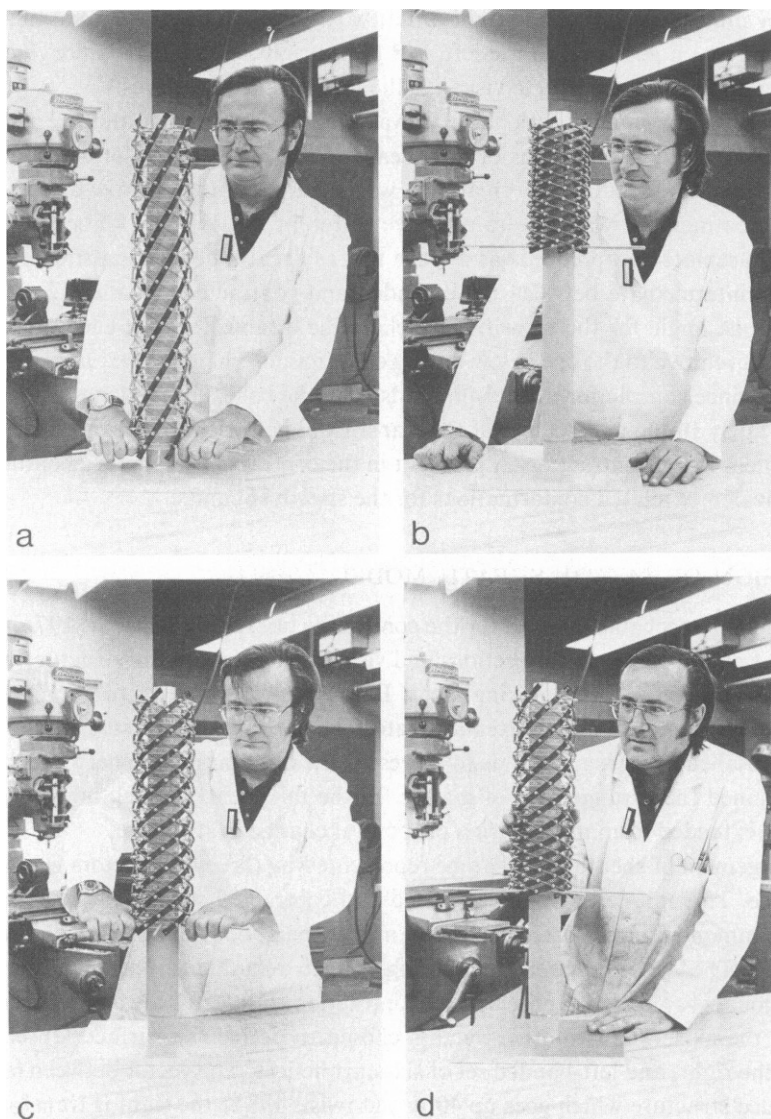


**Figure 12** Charles Ingersoll, Jr. demonstrating four states of the contractile model representing the arrangement and energetic relation of the subunit in bacteriophage T4 tail sheath. (a) Fully extended; (b) fully contracted; (c) partially contracted by releasing tension from the bottom; (d) partially contracted by holding the top portion extended. The scale of the model is 1 in. = 40 Å.

to a length of 24. in. When he releases the end in Fig. 12 *b* the model snaps closed to a contracted length of 9 in. In Fig. 12 *c* he is holding the model at an intermediate extension. All units are equivalently related at the different extensions in Figs. 12 *a*, *b*, and *c*. Even though the coupling is relatively flexible, applying an axial force between opposite ends leads to a uniform separation of the rings. Under these conditions the model behaves synchronously, conserving symmetry according to allosteric precepts. However, when Ingersoll exerts a pull on the middle of the sheath model in Fig. 12 *d* the top is extended and the bottom contracted. There is a gradual contraction gradient between the two ends since the long-range coupling provided by the steel straps will not allow an abrupt transition from the extended to contracted



state. In this condition the layers along the length of the sheath are quasi-equivalently related.

The transition from the contracted to the extended state in Fig. 12 *d* corresponds to the kind of intermediate structures observed by Moody (1973) in partially contracted sheaths. These observations indicate that there are links between the sheath subunits and the central tube which are sequentially released when the contraction is triggered by a structural change in the baseplate. If the sheath were held extended only by the connections with the tube through the base plate at the bottom and by the connections with the adaptor at the top, then contraction should have proceeded synchronously.

Sequential release of the sheath subunits from the tube is illustrated by the sequence of photographs of the model in Fig. 13. Radially elongated sheath subunits are represented by the 144 white knobs attached to metal rods inserted through holes in the lucite rings. In the extended state, the rods are pinned in the grooves of the tube. The baseplate is schematically represented by the metal ring connected to the bottom of the sheath and pinned by six black knobs to the bottom of the tube in Fig. 13 *a*. Release from the base plate initiates the contraction; in Fig. 13 *b*, the baseplate and the bottom five annuli have been unpinned; in succeeding frames six annuli are disconnected at a time up to Fig. 13 *e*, where the contraction is complete. The sequential release was operated manually by pulling out the knobs to make the contraction proceed in discrete steps for photography. By tapering the grooves on the tube, the release could be made automatic, driven by the springs contracting the structure. It is evident from the sequence of pictures that the extent of contraction is a nonlinear function of the number of annuli released: the structure is about half-contracted when two-thirds of the units have been disconnected from the tube. Contraction is coupled with rotation of the tube.

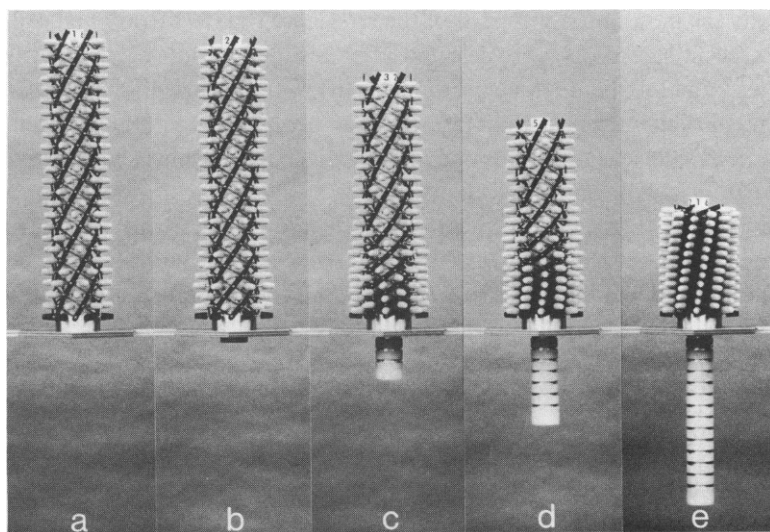


Figure 13 Steps in the contraction of the T4 tail sheath model. The radially elongated units can be pinned or unpinned from the grooves in the tube. In the fully extended model (*a*) all 144 sheath units represented by white knobs and 6 black connector units of the baseplate are pinned to grooves in the tube; in (*b*) baseplate units and the sheath units in the first 5 annuli have been disconnected from the tube; in (*c*) 11 annuli have been disconnected; in (*d*) 17 annuli have been disconnected; in (*e*) the contraction is complete and only the 24th annulus remains connected to the tail tube. The numbers on the top of the tube are spaced  $60^\circ$  apart and show the rotation of the tube which is coupled to the contraction of the sheath.

The numbers 1–6 equally spaced around the top of the tube indicate the extent of rotation. As the sheath contracts to three-eighths of its initial length, the tube is screwed in by one complete turn and five-eighths of its total length.

The stages in contraction of the model in Fig. 13 correspond with those experimentally defined for the tail sheath contraction by Moody. The model provides, therefore, a plausible representation of the way energy is stored in the extended structure and the way it is released by the coordinated interactions among the units. The self-controlled switching of this structure illustrates basic design principles (Caspar and Cohen, 1969) which apply to the operation of other biological displacive transitions from simple allosteric enzymes to complex cellular structures.

#### ADAPTATION IN MODELING THE TAIL SHEATH

Charles Ingersoll, Jr. started the construction of the tail sheath model with fabrication of the 24 3/8 in. wide rings that were cut from 4 in. OD, 3 1/2 in. ID lucite tubing. An indexing head was used for drilling the 6 hexagonally arrayed 3/16 in. diameter holes to hold the pins that would fasten each ring to the tail tube; and midway between the first set of holes, another hexagonally arranged set of 6 were drilled for the 4–40 machine screws to fasten the straps and springs. More effort was required to make these rings than for any other component. Until the model was assembled there was no obvious way to test these rings, nor were there any readily available alternatives with which they could be compared. The lucite rings have proved to be the most unsatisfactory part of the model. With the strains experienced during the unpinning and contraction illustrated in Fig. 13, the lucite has started to crack. In retrospect, we can see that aluminum rings should have been used, but lucite was chosen for its transparency and light weight, which does not compensate for its mechanical weakness.

Dynamically the most important parts of the model are the steel straps and coil springs; the components used in the model were selected after testing various alternatives. Steel baling straps and then band saw blade stock (without teeth) were first tried for the invariant length, 6-start helical connections, but both deformed when bent, although they differed in stiffness. A roll of tempered steel spring stock found in the University machine shop proved to have the desired properties: it withstands deformation; it is stiff enough to provide strong coupling between neighboring rings, but elastic enough to allow a gradient in contraction. This moderate-range quasi-coupling between the annuli is an intriguing aspect of the actual structure and of the model built to represent it. If the coupling among the layers were very tight, like the connections in a pair of lazy tongs, the sheath would have contracted synchronously, conserving symmetry. If the coupling were very weak, for example, if each segment of the right-handed helices connecting between layers were separately articulated, then the layers could have switched sequentially with a sharp discontinuity between contracted and uncontracted domains. Success in modeling the quasi-equivalent, graded coupling between the layers was not the result of careful planning in the initial design; rather, the initial design was vague enough to require some trial-and-error testing to find suitable components.

As spacers to keep the coil springs clear of the spring steel straps, electrical stand-offs, 1/4 in. diameter by 1/4 in. long proved satisfactory. Coil springs with a 3-lb. pull were first chosen to contract the model. Before assembly of these 144 springs had gone very far it was clear we had made a mistake: a great effort was required to extend the model and there was risk of injury to fingers or modelo when it snapped closed. Switching to springs with a 1-lb. pull solved this problem. The final parts of the model built were the schematic tail tube and the

pins holding the extended sheath to it. Polished 3/16 in. aluminum rods capped with electrical wire nuts provided secure attachments of the sheath to the tube that are easy to release. The tail tube model, consisting of an aluminum tube with 24 grooves spaced 1 in. apart to represent its layers, is enigmatic. How is the tail tube actually constructed and what determines its length? Contemplation of the quasi-equivalent axial relation of the annuli in the contracting sheath model has suggested another way of looking at the length limitation problem.

#### TAIL TUBE LENGTH LIMITATION

Bacteriophage tail structures epitomize the problem of length regulation in linear aggregates of identical units. For all phage tails whose formation has been characterized, a basal structure is necessary to initiate the assembly (Casjens and King, 1975; Eiserling, 1979). Once assembly has started, it proceeds rapidly to form a structure consisting of a fixed number of layers. Terminator proteins add to complete the tail, but if these proteins are missing the tail structure may eventually add on more units. The tail tube of T4 consists of 24 annuli of 6 subunits each (Moody, 1971). Wagenknecht and Bloomfield (1977) have isolated T4 tail tube subunits and the baseplate structure; with this system they have followed the assembly process in vitro. When the tail tube subunits and baseplates are allowed to react over a wide range of initial concentration ratios, the most frequent length observed is the same 24-layer structure formed under normal growth conditions. Some longer tube structures are observed if the tail tube subunits and baseplates are reacted for much longer than an hour. For reaction times less than half an hour the number of assembled complexes is reduced but most of those that are observed have normal length.

Two mechanisms have been proposed to account for the length limitation: either measurement by a length-determining "ruler" (King, 1971); or exhaustion of growth by the build-up of "cumulated strain" (Kellenberger, 1969, 1972). So far no recognizable ruler has been identified. Cumulated strain, which is a version of quasi-periodic axial bonding (Caspar, 1966), simply won't work to define a 24-layer structure precisely. A set of units with bond sites that require different axial separation for optimum bonding could form a quasi-periodic linear aggregate. As more units are combined, progressively greater deformations would be required to form both sets of bonds, thus limiting further association beyond some point. This type of quasi-periodic axial bonding accounts for the stable two-layer disc of TMV protein, and it might work to define a three-layer structure. As the number of layers becomes larger, the steps in the free-energy change become smaller and the size of the aggregates formed will fluctuate. Calculation for a thermodynamic model with an arbitrary linearly increasing strain energy term (Caspar, 1963; Wagenknecht and Bloomfield, 1975) show that the mean length for such a model depends on the bond and strain energy and on the protein concentration. This would not make a very reproducible control mechanism. If we knew how the length of the tail tube were determined (assuming that it is not done with a ruler) it should be possible to build a working length-limiting model.

#### A WORKABLE LENGTH-LIMITING MECHANISM

A workable length-limiting mechanism was suggested by the appearance of the partially contracted tail sheath model in which there is a gradient of quasi-equivalent conformations. A length-limiting mechanism in which there is no direct interaction between the last layer and the first would have to operate on some graded change in structure between consecutive

layers. The baseplate provides an obvious foundation for maintaining a gradient of quasi-equivalently related layers. The baseplate must also serve as the autosteric effector to initiate the change in tail tube subunits from an unsociable to an associable state. When the baseplate structure has "turned on" the first layer, the first layer can then turn on the next and so on.

Let us assume that attaching the first layer to the baseplate requires the layer to be strained into a higher energy conformational state than it was in before attachment. Attachment also activates the latent donor sites on the top of the first layer. The arrangement of these sites is such that, when the second layer is attached to the first, the conformational strain in the second layer is less than that in the first layer. And again for the third layer the strain is less than in the second and so on up to the  $t$ -th layer that fits very comfortably on the  $(t-1)$ th layer. Up to the  $t$ -th layer, each layer binds more strongly than the one before. Thus, once the assembly has started it proceeds rapidly to complete the stack of  $t$  layers. The conformational strain in the layers proximal to the baseplate can be thought of as a pulling apart of some bonded surfaces. In the  $t$ -th layer these bonded surfaces are in close contact. To put a  $(t+1)$ th layer on would then require compression of matter in order to fit the receptor sites to the donor sites on the  $t$ -th layer. The positive free energy change for this forcing together more than offsets the decrease on free energy for forming another set of axial bonds. Therefore, assembly stops at the  $t$ -th layer.

The next step is the binding of a terminator complex that is specific for the disposition of the donor sites on the  $t$ -th layer but which cannot be stretched to fit on any of the more proximal layers. When the terminator binds, it induces a local structural change in the  $t$ -th layer which, in turn, induced a structural change in the  $(t-1)$ th layer and so on down to the baseplate. When the baseplate receives this signal, it then relaxes into a state where the strain on the first layer is removed. The relaxation of the first layer leads to the relaxation of the second layer and so on. At the end of this process, the tube layers are all equivalently related. If the terminator is then removed and the tube depolymerized, the tube units will come off in a relaxed, associable state rather than their initial repressed, unsociable state. Changing conditions to favor repolymerization of tube units will then lead to the formation of long polytube structures of indeterminate length. Relaxation of the tube structure to this equivalent state may also take place without triggering by the terminator but very slowly because there is an energy barrier for spontaneous switching.

#### PLAN FOR A SELF-LIMITING MODEL

The hypothetical length-limiting mechanism just described is based on the conception of a mechanical model that would behave in this way. For simplicity in construction, this model is designed to have twofold symmetry rather than sixfold for the base and tube layers. There is no loss in generality with this simplification since the length control mechanism visualized would work with any rotational symmetry. Each subunit will have a socket on its lower side and a complementary prong on the upper surface which is retracted in the unsociable state. A pair of springs will link the two units in a dimer holding their apposing faces in contact; and the top and bottom surfaces will be perpendicular to the twofold axis. This system of dimers with prongs retracted will have no affinity for each other.

The planar baseplate structure will have a pair of perpendicularly projecting prongs a distance  $(D+d)$  apart. The separation of the pair of sockets on the bottom side of the stacking dimer unit will be  $D$  when the isolated dimer is at equilibrium with apposing faces in contact. Thus, to fit a dimer onto the baseplate prongs, the dimer pair will have to be stretched by a distance  $d$ , separating the apposing faces by a distance  $d$ . The free energy for attaching this

first layer is  $\Delta G_1 = \Delta G_b + \Delta G_s$ . The bond energy  $\Delta G_b$  is the net free energy change for forming the bonds and is negative. The conformational strain energy,  $\Delta G_s$ , for stretching the distance  $d$  is positive but less than  $-\Delta G_b$ . When the baseplate prongs are inserted into the sockets of the first layer pair, this will trip a catch in each unit that will extend and lock into place the retracted pair of prongs. The distance between the pair of prongs on the top surface of the layer pair is designed to be a distance  $d/(t-1)$  closer together than the sockets on the bottom surface (that are a distance  $D$  apart at equilibrium). When the first layer pair is attached to the base prongs, the extended pair of prongs on the top surface will be a distance  $D + [(t-2)/(t-1)]d$  apart. The free energy change for adding the second layer is then  $\Delta G_2 = \Delta G_b + [(t-2)/(t-1)] \Delta G_s$ . This assumes that the bonds between the first and second layer will have the same energy as those between the base and first layer; and the strain energy will be linear with the extension of the dimer beyond its normal equilibrium separation. By the same argument, the free energy change for adding the  $n$ th layer is  $\Delta G_n = \Delta G_b + [(t-n)/(t-1)]\Delta G_s$ . When  $n = t$ , then  $\Delta G_t = \Delta G_b$ . The pair of units in the top layer,  $t$ , will have their sockets separated by the distance  $D$ . Thus, there will be no strain fitting this layer to the one below. The prongs on the upper surface of the top layer,  $t$ , will be separated by a distance  $D - [1/(t-1)]d$ . Since the model is to be made of incompressible matter, it will be impossible to push a pair of units together to give a separation less than  $D$  between sockets. Therefore, an additional layer cannot attach to the top layer. The  $n$ th layer is always bound more strongly than the  $(n-1)$ th layer up to layer  $t$ . Beyond this point no more units can be added.

At the stage when the top unit has been added, the stack of  $t$  units will form a tapered column: the pair at the top will be in contact on the twofold axis; and the pair on the bottom will have their inner surfaces separated by a distance,  $d$ . The tangent of the angle subtended between the twofold axis and a line along either inner surface of the stack will be  $(d/2(t-1)h)$  where  $h$  is the layer separation. Quasi-equivalent stacking of the layers will occur in this model because their bonding surfaces will be constrained to be perpendicular to the axis of the stack, while the separation of their donor prongs on the top surface is to be a distance  $d/(t-1)$  less than the separation of the receptor sockets on their bottom surface.

The next stage of assembly will be the addition of the terminator structure which has a pair of sockets on its bottom surface separated by  $D - d/(t-1)$ . This separation will be made inextensible and incompressible. The terminator will therefore bind specifically to layer  $t$  but not to any of the previous layers. When the terminator binds to the  $t$ -th layer, it will trip a catch on the top layer which will trip a catch on the layer below which will trip the catch on the next layer and so on, down to the baseplate. Releasing the catch on the baseplate will release a pair of springs that will draw the two halves closer together by a distance  $d$  while at the same time, each half of the baseplate will tilt down by an angle whose tangent is  $(d/2(t-1)h)$ . This relaxing movement of the baseplate will carry the layers of subunits in the same direction forming a stack of blunt, upward facing chevrons. At the end of this process any line connecting identical points on consecutive units will be parallel to the axis of the stack. Thus, all the layer units will then be equivalently related. (Since this relaxation is energetically favored, it may occur spontaneously; but without the help of the terminator structure the activation energy is high so that the rate of spontaneous relaxation is very slow.) If the terminator were removed then layer units could be removed. They will come off in a relaxed associable state since when their prongs were extended they were locked into place by a spring catch. Units in this relaxed associable state can then be added back to form stacks of any length.

In the assembly process of this model the layer dimers will exist in three distinguishable conformation states. Initially, the dimers will be in an unsociable state with prongs retracted and bonding surfaces of the pair of units in the same plane. These pairs will be added to the stack when the baseplate is in its tense state with its two bonding surfaces coplanar. Adding the layer pairs to the stack will switch them into an associable quasi-equivalently related family of states in which the bonding surfaces are perpendicular to the axis of the stack. In this stack there will be  $t$  quasi-equivalent conformation whose energies range from  $\Delta G_i = \Delta G_b + \Delta G_s$  to  $\Delta G_i = \Delta G_b$ . After the terminator has been added, the layer units will all be switched into a relaxed associable state with all units equivalent regardless of their position in the stack. If evidence for other conformational states of the T4 tail tube subunits is uncovered, it should be possible to represent such states by an extension of the design scheme described here. Construction of this model has been planned to analogize in a simple mechanical system the control mechanisms that may operate to limit the length of the tail tube assembly; but no representation is intended of the actual structures and movements that occur in the tail tube assembly process. Comparing the switching mechanisms to be employed in this model with those experimentally recognized in the switching steps for TMV assembly, Nature's mechanisms seem yet more intricately purposeful than the fanciful (but pragmatically restricted) ones envisaged here. The design of the mechanical model has been constrained by the condition that a working model could be built using the technology available in our machine shop. The next step is to build the model.

#### ANTICIPATION

Asking a meaningful new question presumes anticipation of the unforeseen answer. Analogy is an anticipatory link in this proleptic process. Konrad Lorentz (1974) assures us that "no such thing as a false analogy exists: An analogy can be more or less detailed and hence more or less informative." The aptness of a mechanical analog intended to exemplify purposeful movement in the assembly or action of a vital structure can be judged by how well it works. How informative a working analog will be depends on how much relevant information has been inadvertently carried over from the technology, art or science used in its conception and construction. This kind of information can constitute answers to questions not yet asked.

Faced with the same answer, enquiring minds may ask different questions. Buckminster Fuller rediscovered the cuboctahedron as the coordination polyhedron in cubic close-packing and renamed it the "vector equilibrium" (Marks, 1960). Visualizing this figure not as a solid but as a framework of edges connected at the vertices, he transformed the square faces into pairs of triangles to form an icosahedron; and subtriangulation of the spherical icosahedron led to Geodesic domes. Some of the icosageodesic designs used by Fuller for his domes have also been used for centuries in the Far East for weaving coolie hats (cf., Pawley, 1962). Goldberg (1937), unnoticed, had enumerated all the possible icosahedral surface lattices as a mathematical curiosity, and this enumeration was discovered again to explain why isometric viruses have icosahedral symmetry (Caspar and Klug, 1962). While attempting to account for the form of the six-cornered snowflake, Johannes Kepler (1611) digressed to enquire why pomegranate seeds have the shape of the rhombic dodecahedron, which led to his discovery of cubic close-packing: the seeds, initially small spheres, will close-pack and as they grow they will squeeze each other into this polyhedral shape because this is the space-filling solid for the cubic close-packed lattice. J.D. Bernal (1960) reinvented the pomegranate to explore random close-packing of spheres as a model for the structure of liquids. He squeezed together in a bag many little equal size spheres of plasticine coated with chalk dust to form a mass of randomly

close-packed space-filling polyhedra. Breaking apart this mass he counted faces and edges of the irregular polyhedra: the most common number of faces is 13 and the most common number of sides to a face is 5 instead of the 12 regular 4-sided faces of Kepler's rhombic dodecahedron. Whether or not the packing of pomegranate seeds was Kepler's clue for discovery of cubic close-packing his conclusion about the shape of these seeds recognizes a fundamental relation in the genesis of form of all living structures: "The demands of their matter coincide with the proportions of their growth."

The demands of matter for a protein molecule are genetically predetermined but the proportions of growth for associable proteins leave room for some vital indeterminacy within the self-controlled behavior of the group. Quasi-equivalent conformations of the structural protein in an icosahedral virus capsid represent a kind of frozen-in motion that can indicate variable and invariant parts of the structure. A key movement for structural proteins appears to be a self-controlled switching from an unsociable to an associable conformation. This process is homologous with allostery (Monod, Wyman and Changeux, 1965) and is called autostery here to emphasize the homology. Energy to drive the change from the unsociable to the intrinsically less stable associable conformation is provided by the intersubunit bonds. Thus, the growing structure acts as the autosteric effector to control its own assembly. A gradient of quasi-equivalent conformational states in a linearly quasi-periodic assembly can act to precisely limit its size. Protein subunits of a virus particle can function in more than one way and there can be more than one pathway leading to their assembly in the completed structure (Makowski, 1980). In all these self-controlled movements, an anticipation is built into the structure of the proteins, but the particular realization of the inherited potential is a consequence of individual experience.

This paper is a tribute to Lee Makowski: with his understanding help, ideas have been fashioned into text. The models that provide illustration and source of ideas have been built with skill and ingenuity by the late Charles Ingersoll, Sr., Charles Ingersoll, Jr., and John De Roy. William Saunders has artfully photographed the recent models and the resurrected photographs in Fig. 3-6 were taken by Fred Clow. Aaron Klug, together with whom this work started, invented the term "quasi-equivalence," and throughout the years he has been my most valued source of information about structure. R. Buckminster Fuller provided anticipatory design stimulus at a critical time. For help and incentive, I thank Harold Bloom, Penny Caponigro, Gwladys Caspar, Carolyn Cohen, Nancy Crawford, Fred Eiserling, Ken Holmes, Adrian Parsegian, Valerie Parsegian, and Louise Seidel. For over two decades my work on assembly has been supported by the National Cancer Institute, until 1972 at the Children's Cancer Research Foundation with grant CA-04696, and since then at the Rosenstiel Center with grant CA-15469.

*Received for publication 31 March 1980.*

## REFERENCES

- Asakura, S. 1968. A kinetic study of *in vitro* polymerization of flagellin. *J. Mol. Biol.* **35**:237-239.
- Asakura, S., G. Eguichi, and T. Iino. 1964. Reconstruction of bacterial flagella *in vitro*. *J. Mol. Biol.* **10**:42-56.
- Atkinson, D. E. 1977. Cellular Energy Metabolism and Its Regulation. Academic Press, Inc., New York.
- Bancroft, J. E. 1970. The self-assembly of spherical plant viruses. *Adv. Virus Res.* **16**:99-134.
- Bernal, J. D. 1960. The structure of liquids. *Sci. Amer.* **203**:124-134.
- Butler, P. J. G., and A. Klug. 1971. Assembly of the particle of tobacco mosaic virus from RNA and disks of protein. *Nat. New Biol.* **229**:47-50.
- Butler, P. J. G., J. T. Finch, and D. Zimmern. 1977. Configuration of tobacco mosaic virus RNA during virus assembly. *Nature (Lond.)* **265**:217-219.
- Casjens, S., and J. King. 1975. Virus assembly. *Annu. Rev. Biochem.* **44**:555-604.
- Caspar, D. L. D. 1963. Assembly and stability of the tobacco mosaic virus particle. *Adv. Protein Chem.* **18**:37-118.
- Caspar, D. L. D. 1966. Design and assembly of organized biological structures. In *Molecular Architecture in Cell Physiology*. T. Hayashi and A. Szent-Gyorgyi, editors. Prentice-Hall, Inc., Englewood Cliffs, N. J. 191-207.
- Caspar, D. L. D., and C. Cohen. 1969. Polymorphism of tropomyosin and a view of protein function. In *Nobel Symposium II*. A. Engstrom and B. Strandberg, editors. John Wiley & Sons, Inc., New York. 393-414.

- Caspar, D. L. D., and K. C. Holmes. 1969. Structure of Dahlemense strain of tobacco mosaic virus: a periodically deformed helix. *J. Mol. Biol.* **46**:99–133.
- Caspar, D. L. D., and A. Klug. 1962. Physical principles in the construction of regular viruses. *Cold Spring Harbor Symp. Quant. Biol.* **27**:1–24.
- Caspar, D. L. D., and A. Klug. 1963. Structure and assembly of regular virus particles. In *Viruses, Nucleic Acids, and Cancer*. Williams and Wilkins, Baltimore, Md. 27–39.
- Champhess, J. N., A. C. Bloomer, G. Bricogne, P. J. G. Bulter, and A. Klug. 1976. The structure of the protein disk of tobacco mosaic virus to 5 Å resolution. *Nature (Lond.)*. **259**:20–24.
- Cohen, C., and K. C. Holmes. 1963. X-ray diffraction evidence for  $\alpha$ -helical coiled-coils in native muscle. *J. Mol. Biol.* **6**:423–432.
- Cooke, R., and L. Murdoch. 1973. Interaction of actin with analogs of adenosine triphosphate. *Biochemistry*. **12**:3927–3932.
- Crane, H. R. 1950. Principles and problems of biological growth. *The Scientific Mon.* **70**:376–389.
- Crick, F. H. C. 1953. The Fourier transform of a coiled-coil. *Acta Cryst.* **6**:685–697.
- Crick, F. H. C., and J. D. Watson. 1956. Structure of small viruses. *Nature (Lond.)*. **177**:473–475.
- Durham, A. C. H., and A. Klug. 1971. Polymerization of tobacco mosaic virus protein and its control. *Nat. New Biol.* **229**:42–46.
- Eiseling, F. A. 1979. Bacteriophage structure. In *Comprehensive Virology*. **13**:543–580.
- Fraenkel-Conrat, H., and R. C. Williams. 1955. Reconstitution of active tobacco mosaic virus from its inactive protein and nucleic acid components. *Proc. Natl. Acad. Sci. U.S.A.* **41**:690–698.
- Goldberg, M. 1937. A class of multi-symmetric polyhedra. *Tohoku Math. J.* **43**:104–108.
- Harrison, S. C., A. J. Olson, C. E. Schutt, F. K. Winkler, and G. Bricogne. 1978. Tomato bushy stunt virus at 2.9 Å resolution. *Nature (Lond.)*. **276**:368–373.
- Hayashi, T., and R. Rosenbluth. 1960. Studies on actin. II. Polymerization and the bound nucleotide. *Biol. Bull.* **119**:290.
- Hohn, T., and B. Hohn. 1970. Structure and assembly of simple RNA bacteriophages. *Adv. Virus Res.* **16**:43–98.
- Holmes, K. C., G. J. Stubbs, E. Mandelkow, and U. Gallwitz. 1975. Structure of tobacco mosaic virus at 6.7 Å resolution. *Nature (Lond.)*. **254**:192–196.
- Hsu, C. H., J. A. White, and O. P. Sehgal. 1977. Assembly of southern bean mosaic virus from its two subviral intermediates. *Virology*. **81**:471–475.
- Kamb, B. 1968. Ice polymorphism and the structure of water. In *Structural Chemistry and Molecular Biology*. A. Rich and N. Davidson, editors. W. H. Freeman Co., San Francisco, Calif. 507–542.
- Kellenberger, E. 1969. Polymorphic assemblies of the same major virus protein subunit. In *Nobel Symposium II*. A. Engstrom and B. Strandberg, editors. John Wiley and Sons, New York. 349–366.
- Kellenberger, E. 1972. Mechanisms of length determination in protein assemblies. *Ciba Fdn. Symp.* **7**:295–299.
- Kepler, J. 1611. *De Niue Sexangula*. Godfrey Tampach. Frankfurt am Main. Republished 1966. The Six-Cornered Snowflake. Clarendon Press, Oxford.
- Kikuchi, Y., and J. King. 1975. Genetic control of bacteriophage T4 baseplate morphogenesis. I. Sequential assembly of the major precursor *in vivo* and *in vitro*. *J. Mol. Biol.* **99**:645–672.
- King, J. 1971. Bacteriophage T4 tail assembly: four steps in core formation. *J. Mol. Biol.* **58**:693–709.
- King, J., and N. Mykolajewycz. 1973. Bacteriophage T4 tail assembly: proteins of the sheath, core and baseplate. *J. Mol. Biol.* **75**:339–358.
- Krimm, S., and T. E. Anderson. 1967. Structure of normal and contracted tail sheaths of T4 bacteriophage. *J. Mol. Biol.* **27**:197–202.
- Lebeurier, G., A. Nicolaieff, and K. E. Richards. 1977. Inside-out model for self-assembly of tobacco mosaic virus. *Proc. Natl. Acad. Sci. U.S.A.* **74**:149–153.
- Lorentz, K. Z. 1974. Analogy as a source of knowledge. *Science (Wash. D. C.)*. **185**:229–234.
- Makowski, L. 1980. Structural studies of the assembly of simple viruses. (To appear In *Biological Recognition and Assembly*. Alan R. Liss, Inc., New York.)
- Mandelkow, E., K. C. Holmes, and U. Gallwitz. 1976. A new helical aggregate of tobacco mosaic virus protein. *J. Mol. Biol.* **102**:265–285.
- Mannherz, H. G., H. Brehme, and U. Lamp. 1975. Depolymerisation of F-actin to G-actin and its repolymerisation in the presence of analogs of adenosine triphosphate. *Eur. J. Biochem.* **60**:109–116.
- Marks, R. W. 1960. *The Dymaxion World of Buckminster Fuller*. Reinhold Publishing Corp., New York.
- McLachlan, A. D., and M. Stewart. 1975. Tropomyosin coiled-coil interactions: evidence for an unstaggered structure. *J. Mol. Biol.* **98**:293–304.
- Monod, J., J. Wyman, and J.-P. Changeux. 1965. On the nature of allosteric transitions: a plausible model. *J. Mol. Biol.* **12**:88–188.
- Moody, M. F. 1967a. Structure of the sheath of bacteriophage T4. I. Structure of the contracted sheath and polysheath. *J. Mol. Biol.* **25**:167–200.



- Moody, M. F. 1967b. Structure of the sheath of bacteriophage T4. II. Rearrangement of the sheath subunits during contraction. *J. Mol. Biol.* **25**:201–208.
- Moody, M. F. 1971. Structure of the T2 bacteriophage tail-core, and its relation to the assembly and contraction of the sheath. In First European Biophysics Congress. Wiener Medizinische Akademie, Vienna. 543.
- Moody, M. F. 1973. Sheath of bacteriophage T4. III. Contraction mechanism deduced from partially contracted sheaths. *J. Mol. Biol.* **80**:613–635.
- Oosawa, F., and M. Kasai. 1962. A theory of linear and helical aggregations of macromolecules. *J. Mol. Biol.* **4**:10–21.
- Pauling, L. 1960. The Nature of the Chemical Bond. Cornell University Press, Ithaca, New York. 3rd edition. Chapter 12.
- Pauling, L., and R. B. Corey. 1953. Compound helical configurations of polypeptide chains: structure of proteins of the  $\alpha$ -keratin type. *Nature (Lond.)*. **171**:59.
- Pawley, G. S. 1962. Plane groups on polyhedra. *Acta Cryst.* **15**:49–53.
- Perutz, M. F. 1970. Stereochemistry of cooperative effects in haemoglobin. *Nature (Lond.)*. **228**:726–734.
- Poglazov, B., and T. Nikolskaya. 1969. Self-assembly of the protein of bacteriophage T2 tail cores. *J. Mol. Biol.* **43**:231–233.
- Rayment, I., J. E. Johnson, and M. G. Rossmann. 1979. Metal-free southern bean mosaic virus crystals. *J. Biol. Chem.* **254**:5243–5245.
- Suck, D., I. Rayment, J. E. Johnson, and M. G. Rossmann. 1978. The structure of southern bean mosaic virus at 5 Å resolution. *Virology*. **85**:187–197.
- Vogel, D., G. D. deMarillac, and L. Hirth. 1979. Size distribution in the higher stages of polymerization of the A-protein of tobacco mosaic virus. *Z. Naturforsch.* **34**:782–792.
- Wagenknecht, T., and V. A. Bloomfield. 1975. Equilibrium mechanisms of length regulation in linear protein aggregates. *Biopolymers*. **14**:2297–2309.
- Wagenknecht, T., and V. A. Bloomfield. 1977. *In vitro* polymerization of bacteriophage T4D tail core subunits. *J. Mol. Biol.* **116**:347–359.
- Wegner, A. 1976. Head to tail polymerization of actin. *J. Mol. Biol.* **108**:139–150.
- Wegner, A., and J. Engel. 1975. Kinetics of the cooperative association of actin to actin filaments. *Biophys. Chem.* **3**:215–225.

## DISCUSSION

*Session Chairman:* David Eisenberg *Scribe:* Andrew W. Fulmer

D. EISENBERG: We have an extended comment from Jonathan King.

J. KING: I would like to summarize some of the ideas on self-regulation, referring to the data of Asakura et al. (1964) on bacteria flagella assembly as well as Bloomfield's data on the assembly of bacteriophage T4 tail tube. Flagellin subunits are synthesized inside the bacteria on the ribosomes. Spontaneous polymerization to flagellin polymers inside the bacterium would be disastrous. Thus, they must come off the ribosome in an inactive state which is incapable of polymerization. They can polymerize only on the growing tips of the flagella.

I have represented these inactive subunits with active sites which are buried. They have no tendency to bind to each other. The key point here, which Dr. Caspar makes in his paper, is that these inactive subunits are not in equilibrium with the active state. They are not switching back and forth between the active and inactive states free in solution. Preparations of these subunits will remain stable for several weeks in the unpolymerized state. Free, inactive, subunits are bound only to a reactive initiation structure. Polymerization now pauses, because these subunits are not reactive. Subsequent addition of free subunits can occur only after these initially bound subunits have completed a conformational change. This conformational transition can occur only on the bound surface.

Asakura and his colleagues and Uratani et al. (1972) have shown that this transition was the rate-limiting step in flagellar assembly which took ~0.3 s at 37°C. Once this subunit has switched over to the active state, a new site is generated which binds another free subunit from solution. The newly bound subunit must then be switched over to the active state by the whole organized structure. This cycle is repeated until a fully polymerized structure is formed.

This model assures that the only place where subunits will polymerize is at the site of the initiation structure (King, 1980). Location of the (nonrepetitive) structure allows specific placement of repeating structures in the cell. Without such a control mechanism, one would observe spontaneous polymerization of newly assembled subunits which could not be specifically located within the cell.

The initiation complex for bacterial flagella is a very complex machine which is located in the plasma membrane, while, for bacteriophage T4, it is a baseplate which consists of 15 different structural proteins (Kiruchi and King

[1975]). As Dr. Caspar has pointed out, cooperative polymerization may be described mathematically by nucleation theory. However, this is not what is going on here. This is not a statistical problem of subunits finding one another. There is a very high energy barrier for these subunits to switch over to the active state when free in solution. This energy barrier is overcome by the organized structure which presents a different environment, a catalytic surface, capable of switching the subunit.

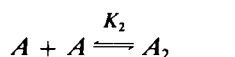
## REFERENCES

- King, J. 1980. Self-regulated assembly of proteins as revealed in phage morphogenesis. *In* Biological Regulation and Development. R. Goldberger, editor. Plenum Press, New York. Vol. II.
- Uratani, Y., S. Asakura, and K. Inahori. 1972. A circular dichroism study of Salmonella flagellin: evidence for conformational change on polymerization. *J. Mol. Biol.* **123**:115-128.

D. EISENBERG: We have another extended comment, from Harold Erickson.

ERICKSON: Dr. Caspar, you have elaborated on the concept of autostery to explain the extreme cooperativity that is observed for macromolecular assemblies such as actin. I would like to sketch out a simple theory that accounts for cooperativity in any assembly which involves two or more bonds between subunits. I will consider the data on the assembly of actin which illustrates how cooperativity can arise without a requirement for special mechanisms.

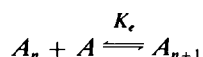
This problem was encountered by Wegner and Engel (1975) in their study on homogeneous nucleation and elongation of actin. They found that the association of actin subunits to form the first dimer was extremely unfavorable,



$$K_2 = 4 \times 10^{-2} \text{ M}^{-1}$$

$$\Delta G_2 = +2 \text{ kcal/mol}$$

while the addition of subsequent subunits (elongation) was extremely favorable;



$$K_e = 1.7 \times 10^5 \text{ M}^{-1}$$

$$\Delta G_e = -7 \text{ kcal/mol}$$

Wegner and Engel suggested that the large difference between the association constant for formation of the first dimer and the association constant for subsequent elongation steps required a special mechanism such as the one which you have described here under the term autostery.

I will show how this cooperativity can be accounted for without invoking a conformational change. The basis for this model is to treat an entropic term as an explicit parameter which is equal to the loss of free energy upon incorporation of a free subunit into the polymer.

This is illustrated by representing the actin polymer as a chain of subunits connected by two types of bonds. One type of bond is represented by bond energy  $e_a$ , the other by  $e_b$ . Formation of the first dimer involves only an  $a$  type of bond, while all subsequent subunits form both an  $a$  and a  $b$  type bond. The key point now is to divide the free energy of association into two parts. One part is the favorable bond energy,  $e_a$  or  $(e_a + e_b)$ , which depends on the number of bonds formed. The other, unfavorable, part is the free energy corresponding to the loss of translational and rotational entropy of the free subunit, which is denoted  $e_s$ . I will assume that the numerical value of  $e_s$  is  $\sim 14$  kcal/mol and is independent of the total number of bonds formed. Now we can write the free energy for formation of the first dimer as,  $\Delta G_2 = -e_a + e_s$ ; for  $\Delta G_2 = +2$  kcal/mol and  $e_s = 14$  kcal/mol  $e_a = 12$  kcal/mol. Similarly, for elongation, where two bonds are formed,  $\Delta G_e = -e_a - e_b + e_s$ , so  $e_b = 9$  kcal/mol.

So what we have done here? I have used a reasonable value for the entropic free energy and the values for  $K_2$  and

$K$ , determined by Wegner and Engel (1975) to calculate values for the two bond energies described above. Thus, nucleation and elongation, as well as the extreme cooperativity, are now described as a simple reversible association which is governed only by the two bond energies and a large entropic term.

As a final and more general point, I think that the theoretical model of Eaton and his colleagues (Ferrone et al., this Discussion), as well as my own unpublished work on microtubule assembly, show that homogenous nucleation is a thermodynamically sound explanation for at least some biological assemblies. Cooperativity is a natural consequence of treating the entropic term explicitly. The cooperativity is actually so extreme that we may need a mechanism of "anti-autostery" to stabilize small intermediates and favor nucleation.

CASPAR: I worked out this same model in 1963 (Caspar, 1963) when trying to analyze the assembly of TMV protein, and arrived at the same conclusion: the entropic term is very large. However, the model just did not work. Also, there is a small error which you made in your model by neglecting the configurational entropy of dimers, trimers, etc. Such considerations suggest that the  $\Delta S$  term is not independent of the size of the polymer. The general point is that the cooperativity arises from one free energy term which is a function of the number of bonds and from another free energy term which is a function of the number of subunits. My description in terms of a conformational energy change is formally the same as a change in configurational entropy of the system. However, the reason for thinking that a conformational energy change is significant is the very direct and compelling experimental evidence for these conformational changes. The conformation of actin in F-actin has been demonstrated to be different from that of G-actin by spectroscopic techniques. This is supported in particular, by the experiments of Asakura (1968) on the assembly of bacteria flagellin. Here, a very large activation energy for the switching from the unassociable state to the associable state of flagellin was measured. The relaxation time for this transition was found to be  $\sim 0.3$  s. We do not know how much the configurational entropy actually contributes to these processes.

BUTLER: I don't think that configurational entropy can be the only mechanism. In 1972, we analyzed the mixture of lengths in growing TMV protein helices. Similar but more detailed measurements have since been made by Schuster and coworkers. The point is that you can have a system which requires a minimum nucleus with a barrier to nucleation. Here, you find polymers of only intermediate sizes which are not closed aggregates, which will then form very long rods only after you change solution conditions. You must allow for some kind of end deformation to stabilize intermediate-sized aggregates. The system does not contain a mixture of only monomers and very long rods under these well-controlled conditions.

CASPAR: Back in that 1963 paper I suggested that there are six or seven different conformational states for TMV protein. I still believe this.

ERICKSON: One of my points was that this entropic parameter certainly cannot be the only explanation. In my own work I find a need for modulating the cooperativity. I do think, however, that models of homogeneous nucleation are an important place to start looking.

SIMON: Measurement of the enthalpy and free energy of activation for the polymerization rate may serve to test the validity of a model such as that described by Dr. Erickson. Such measurements have been performed by Hofrichter, Ross, and Eaton for the case of deoxyhemoglobin S polymerization. If nucleus formation is assumed to involve a constant loss of entropy but an increasing number of bonds formed with addition of each subunit, then the apparent nucleus size, or "cooperativity of nucleation", will always be smaller when derived from the enthalpy of activation alone than when derived from the total free energy of activation measured from polymerization rates. On the other hand, this relationship need not hold for "autostery" models. Unfortunately, such measurements of activation parameters are not available for many other polymerizing systems. This test assumes that polymerization may be approximated by formation of a single nucleus species through a series of decreasingly unfavorable subunit additions, followed by elongation of the nucleus through favorable subsequent addition of subunits; it also assumes that the measured enthalpies associated with nucleus formation and overall polymerization are not markedly perturbed by effects of nonideality.

POTSCHKA: I would like to add one point to the question of binding concepts. Some systems may be very tightly linked to ligand binding, such as proton binding. Electrostatic repulsion may play a dominant role in creating differences in stability and mediating conformational changes. The mechanical picture of a conformational change may be energetically linked to ligand binding in switching from one state to another.

CASPAR: Again, in my 1963 paper I showed that the assembly of TMV protein was controlled by ligand linked proton binding. The protein in the assembled state has some proton binding groups with abnormally high affinity. The process of assembly can be very highly cooperatively linked to the proton binding.

ENGELBORGH: May I ask Dr. Erickson where he gets his numerical value of 14 kcal/mol for  $e_s$ ? Previous reports have ranged from 3–7 kcal/mol. Of course, the higher  $e_s$ , the higher the cooperativity.

ERICKSON: It might be best to treat this as an adjustable parameter.

J. KING: I am concerned about reaching generalizations from the sickling of hemoglobin, which is an aberrant polymerization and is not controlled by the cell. It does not have any of the specificity of the structure formation process built into it. This should be set apart from the polymerization reactions which are designed to form very specific structures. For example, when one isolates subunits from the T4 tail tube by chemical breakdown, these subunits are in the sticky, or switched, state and will polymerize spontaneously like hemoglobin. Infinitely long tubes are formed in the absence of a specific nucleus. However, when you isolate precursor subunits which have never been a part of the completed structure, then polymerization does not spontaneously proceed in the absence of the specific baseplate nucleus. There is a real difference in these precursor-product relationships. People often isolate subunits by degradation of the polymer. If there are different conformational states, then one does not know *a priori* which conformational state was isolated. This may be a problem in the microtubule studies due to the methods of preparation.

EDELSTEIN: If cooperativity of assembly is dominated by entropy, then one would expect a temperature coefficient different from that observed for microtubules and hemoglobin. These systems are cold labile.

ERICKSON: One cannot make direct measurements in solution because the entropy effects from the subunits are totally masked by solvent entropy effects from the hydrophobic bonding. These solvent entropy effects were included in my bond energies,  $e_a$  and  $e_b$ .